

**MINISTÉRIO DA EDUCAÇÃO**

**UNIVERSIDADE FEDERAL DO RIO GRANDE DO SUL**

Escola de Engenharia

Programa de Pós-Graduação em Engenharia  
de Minas, Metalúrgica e de Materiais  
PPGEM

**Avaliação da estabilidade térmica e da cinética de degradação da  
madeira através da caracterização de seus componentes**

Matheus Poletto

Tese para a obtenção do título de Doutor em Engenharia

Porto Alegre

2014

**MINISTÉRIO DA EDUCAÇÃO**

**UNIVERSIDADE FEDERAL DO RIO GRANDE DO SUL**

Escola de Engenharia

Programa de Pós-Graduação em Engenharia  
de Minas, Metalúrgica e de Materiais  
PPGEM

**Avaliação da estabilidade térmica e da cinética de degradação da  
madeira através da caracterização de seus componentes**

Matheus Poletto  
Engenheiro Químico

Tese realizada no Departamento de Materiais da Escola de Engenharia da UFRGS, dentro do Programa de Pós-Graduação em Engenharia de Minas, Metalúrgica e de Materiais – PPGEM, como parte dos requisitos para a obtenção do título de doutor em Engenharia.

Área de Concentração: Ciência dos Materiais

Porto Alegre

2014

Esta tese foi julgada adequada visando o Título de Doutor em Engenharia, área de concentração de Ciência dos Materiais, e aprovada em sua forma final pelos Orientadores e pela Banca examinadora do Programa de Pós-Graduação em Engenharia de Minas, Metalúrgica e Materiais.

Orientadora: Dra. Ruth Marlene Campomanes Santana

Co-orientador: Dr. Ademir José Zattera

Banca Examinadora:

---

Prof. Dr. Marcelo Massayoshi Ueki - UFS

---

Prof. Dr. Marcelo Godinho - UCS

---

Prof. Dr. Carlos Arthur Ferreira - UFRGS

---

Prof. Dr. Telmo Roberto Strohaecker  
Coordenador do PPGEM

## ARTIGOS PUBLICADOS EM PERIÓDICOS

Esta tese está baseada nos artigos a seguir:

**ARTIGO I** - Poletto, M., Zattera, A.J., Santana, R.M.C. Structure differences between wood species: evidence from chemical composition, FTIR spectroscopy, and thermogravimetric analysis. *Journal of Applied Polymer Science*, 126: E337-E344, 2012.

**ARTIGO II** - Poletto, M., Zattera, A.J., Forte, M.M.C., Santana, R.M.C. Thermal decomposition of wood: influence of wood components and cellulose crystallite size. *Bioresource Technology*, 109: 148-153, 2012.

**ARTIGO III** - Poletto, M., Zattera, A.J., Santana, R.M.C. Thermal decomposition of wood: kinetics and degradation mechanisms. *Bioresource Technology*, 126: 7-12, 2012.

## OUTROS ARTIGOS PUBLICADOS

### PERIÓDICOS

Poletto, M., Pistor, V., Zattera, A.J., Santana, R.M.C. Materials produced from plant biomass. Part II: evaluation of crystallinity and degradation kinetics of cellulose. *Materials Research*, 15(3): 421-427, 2012.

Poletto, M., Zattera, A.J., Santana, R.M.C. Effect of natural oils on the thermal stability and degradation kinetics of recycled polypropylene wood flour composites. *Polymer Composites*. Aceito.

Poletto, M., Zattera, A.J., Santana, R.M.C. Thermal stability of recycled polypropylene wood flour composites using natural oils as coupling agents. *SPE Plastics Research Online*. Aceito.

### CONGRESSOS

Poletto, M., Zattera, A.J., Santana, R.M.C. Influência do teor de extrativos na estabilidade térmica de duas espécies de madeira. In: 12 Congresso Brasileiro de Polímeros (12 CBPol), 2013, Florianópolis.

Poletto, M., Zattera, A.J., Santana, R.M.C. Efeito da adição de ácidos carboxílicos como compatibilizantes nas propriedades mecânicas e morfológicas de compósitos de PPr reforçado com pó de madeira. In: 12 Congresso Brasileiro de Polímeros (12 CBPol), 2013, Florianópolis.

Poletto, M., Junges, J., Zattera, A.J., Santana, R.M.C. Efeito da utilização de ácidos orgânicos como agentes compatibilizantes em compósitos de PPr/pó de madeira. In: 20 Congresso Brasileiro de Engenharia e Ciência dos Materiais, 2012, Joinville.

Poletto, M., Junges, J., Zattera, A.J., Santana, R.M.C. Influencia de la adición de agentes compatibilizantes provenientes de recursos renovables en las propiedades mecánicas, térmicas y morfológicas de los compuestos PP/harina de madera. In: XIII Simposio Latinoamericano de Polímeros - SLAP 2012, 2012, Bogotá.

Poletto, M., Zattera, A.J., Forte, M.M.C., Santana, R.M.C. Influence of extractive content on wood flour thermal stability of different wood species from Brazil. In: The Polymer Processing Society - 27 th Annual Meeting, 2011, Marrakech.

Poletto, M., Schneider, V.E., Zattera, A.J., Santana, R.M.C. Geração de resíduos poliméricos e de resíduos de madeira no município de Caxias do Sul e as perspectivas de aproveitamento. In: 26º Congresso Brasileiro de Engenharia Sanitária e Ambiental, 2011, Porto Alegre.

## EPÍGRAFE

“A mente que se abre a uma nova ideia jamais voltará ao seu tamanho original.”

Albert Einstein

## AGRADECIMENTOS

À professora Dra. Ruth Marlene Campomanes Santana pela orientação durante a realização deste trabalho.

Ao professor Dr. Ademir J. Zattera pela co-orientação durante a construção deste trabalho.

À bolsista Janaína Junges pelo auxílio na caracterização dos materiais estudados.

Aos professores do PPGEM e NTPOL-UCS por compartilharem seu conhecimento, auxiliando na minha qualificação profissional.

Aos colegas do NTPOL-UCS Heitor L. Ornaghi Júnior, Diego Piazza, Tomas Polidoro e todos os outros doutorandos, mestrandos e bolsistas.

Aos técnicos do Laboratório de Polímeros da UCS pelo auxílio na realização das análises para caracterização das amostras.

Ao Prof. Dr. Ricardo Campomanes Santana pelo envio das amostras de madeiras provenientes do Mato Grosso.

A todos que, de alguma forma, auxiliaram na elaboração deste trabalho.

# SUMÁRIO

<b>SUMÁRIO</b> .....	<b>i</b>
<b>ÍNDICE DE FIGURAS</b> .....	<b>ii</b>
<b>ÍNDICE DE TABELAS</b> .....	<b>iii</b>
<b>SIGLAS E ABREVIATURAS</b> .....	<b>iv</b>
<b>RESUMO</b> .....	<b>v</b>
<b>ABSTRACT</b> .....	<b>vi</b>
<b>1 INTRODUÇÃO</b> .....	<b>1</b>
1.1 OBJETIVO.....	3
1.1.1 <i>Objetivo geral</i> .....	3
1.1.2 <i>Objetivos específicos</i> .....	3
1.2 JUSTIFICATIVA.....	3
<b>2 REVISÃO BIBLIOGRÁFICA</b> .....	<b>5</b>
2.1 MADEIRA.....	5
2.1.1 <i>Composição química da madeira</i> .....	5
2.1.2 <i>Resíduos de madeira</i> .....	9
2.2 CARACTERÍSTICAS DA MADEIRA E DE SEUS COMPONENTES.....	11
2.3 CINÉTICA DE DEGRADAÇÃO DA MADEIRA.....	12
2.3.1 <i>Energia de ativação</i> .....	12
2.3.2 <i>Mecanismo de degradação</i> .....	13
<b>3 MATERIAIS E MÉTODOS</b> .....	<b>14</b>
3.1 ESPÉCIES DE MADEIRA.....	14
3.2 DETERMINAÇÃO DOS COMPONENTES DA MADEIRA.....	14
3.3 ESPECTROSCOPIA NO INFRAVERMELHO COM TRANSFORMADA DE FOURIER (FTIR).....	14
3.4 DIFRAÇÃO DE RAIOS-X (DRX).....	15
3.5 ANÁLISE TERMOGRAVIMÉTRICA.....	15
<b>4 ARTIGOS PUBLICADOS</b> .....	<b>16</b>
4.1 CAPÍTULO 1 – ARTIGO I.....	16
4.2 CAPÍTULO 2 – ARTIGO II.....	24
4.3 CAPÍTULO 3 – ARTIGO III.....	30
<b>5 DISCUSSÃO E INTEGRAÇÃO DOS ARTIGOS</b> .....	<b>36</b>
<b>6 CONCLUSÃO</b> .....	<b>41</b>
<b>7 SUGESTÕES PARA TRABALHOS FUTUROS</b> .....	<b>42</b>
<b>8 REFERÊNCIAS</b> .....	<b>43</b>



## ÍNDICE DE FIGURAS

Figura 1: Estrutura celular e componentes principais da madeira [Adaptado 24].	5
Figura 2: Estrutura química do mero da celulose [23,26].	6
Figura 3: Alguns dos componentes da hemicelulose [21-22].	6
Figura 4: Modelo proposto para estrutura química da lignina [28].	7
Figura 5: Destinação dos resíduos de madeira da região amazônica (a) [35] e da Serra Gaúcha (b) [9].	10

## ÍNDICE DE TABELAS

Tabela 1: Terpenos, óleos, ceras e ácidos graxos encontrados em diversas espécies de madeira.....	8
---	---

## SIGLAS E ABREVIATURAS

DIP - *Dipteryx odorata*

D<sub>n</sub> - Mecanismo de degradação por difusão

D3 - Mecanismo de degradação por difusão nas três dimensões

EUG - *Eucalyptus grandis*

FTIR - Espectroscopia no infravermelho com transformada de Fourier

FWO – Método de Flynn-Wall-Ozawa

F1 – Mecanismo de degradação por reação aleatória

HBI - Intensidade de Ligação Hidrogênio

ITA - *Mezilaurus itauba*

LOI - Índice de Ordenamento Lateral

PIE - *Pinus elliottii*

TCI - Índice de Cristalinidade Total

X - Fração de cadeias de celulose contidas no interior dos cristalitos

## RESUMO

Neste trabalho, as relações entre os componentes da madeira, cristalinidade da celulose, influência do teor de extrativos na degradação térmica da madeira, correlação entre a composição química e as propriedades físicas de quatro espécies de madeira foram investigadas através de análises químicas, espectroscopia no infravermelho com transformada de Fourier (FTIR), difração de raios-X e termogravimetria. A influência dos componentes da madeira e da cristalinidade da celulose na degradação térmica da madeira foi também investigada utilizando os métodos de Flynn-Wall-Ozawa e Criado. As espécies estudadas foram *Pinus elliottii* (PIE), *Eucalyptus grandis* (EUG), *Mezilaurus itauba* (ITA) e *Dipteryx odorata* (DIP). As análises químicas mostraram que as espécies DIP e ITA contêm uma quantidade maior de extrativos associadas a menores quantidades de holocelulose e lignina que as espécies PIE e EUG. A espectroscopia no infravermelho demonstrou que a maior quantidade de extrativos na espécie ITA pode estar associada a bandas mais intensas em 2920, 2850 e 1510  $\text{cm}^{-1}$ . Os resultados das análises termogravimétricas demonstraram que elevadas quantidades de extrativos associadas com baixa cristalinidade e menor tamanho de cristalito da celulose podem acelerar o processo de degradação e reduzir a estabilidade térmica da madeira. Por outro lado, os resultados indicaram que a cristalinidade da celulose inibe a degradação da madeira, uma vez que as regiões de celulose organizada retardam o processo de degradação porque as cadeias de celulose mais organizadas impedem a difusão o que aumenta a estabilidade térmica da madeira. O método de Criado mostrou que o mecanismo de degradação da madeira ocorre por processos de difusão quando a conversão é inferior a 40%. Quando a conversão ultrapassa 50% o processo de degradação da madeira é o resultado de uma nucleação aleatória com um núcleo de degradação em cada partícula. Os resultados obtidos indicam que a cristalinidade da celulose afeta a temperatura de degradação térmica e consequentemente a cinética de degradação da madeira.

## ABSTRACT

In this work, the relationship between wood components, wood cellulose crystallinity, influence of extractives on wood thermal degradation, correlation between chemical composition, and physical properties of four wood species were investigated by chemical analysis, Fourier transform infrared (FTIR) spectroscopy, X-ray diffraction, and thermogravimetry. In addition, the influences of wood components and cellulose crystallinity on the wood kinetic degradation were also investigated by using Flynn-Wall-Ozawa and Criado methods. The species studied were *Pinus elliottii* (PIE), *Eucalyptus grandis* (EUG), *Mezilaurus itauba* (ITA) and *Dipteryx odorata* (DIP). The chemical analysis showed that DIP and ITA contain a higher quantity of extractives and lower quantities of holocellulose and lignin than PIE and EUG. FTIR spectroscopy demonstrated that higher extractives content in ITA might be associated with more intense bands at 2920, 2850 and 1510  $\text{cm}^{-1}$ . The thermogravimetric results demonstrated that higher extractives content associated with lower crystallinity and lower cellulose crystallite size can accelerate the degradation process and reduce wood thermal stability. On the other hand, the results indicated that cellulose crystallinity inhibits wood degradation, since organized cellulose regions slow the degradation process because the well-packed cellulose chains impede diffusion, which improves the wood's thermal stability. The Criado method showed that the wood degradation mechanism occurs by diffusion processes when the conversion values are below 40%. When the conversion values are above 50% the degradation of wood is a result of random nucleation with one nucleus in each particle. The obtained results indicated that the cellulose crystallinity affects the thermal degradation temperature and consequently the degradation kinetics of wood.

# 1 INTRODUÇÃO

Nos últimos anos a crescente preocupação da sociedade com as questões vinculadas ao meio ambiente vem impulsionando ações relacionadas com a minimização da geração de resíduos, reciclagem e sustentabilidade em diversos setores industriais. No setor florestal não é diferente. Este segmento é conhecido por utilizar recursos naturais em larga escala e por gerar grandes quantidades de resíduos de madeira [1-3]. Desta forma, as ações ligadas ao reaproveitamento e reciclagem dos resíduos de madeira vêm sendo realizadas por grandes indústrias [4]. Contudo, a abundância de matéria prima em certas regiões do Brasil, como na região amazônica e na Serra Gaúcha, associado à utilização de condições de processamento que geram desperdício contribuem em grande parte com o reduzido aproveitamento da madeira e consequente elevada geração de resíduos.

O percentual de resíduos gerado em relação à quantidade de madeira processada depende, dentre outros fatores, do tipo de processo adotado, do tipo de matéria-prima utilizada, das condições tecnológicas empregadas e do tipo de produto final [5-6]. Nas diversas etapas de processamento da madeira, desde o abate da árvore até a operação de lixamento de qualquer peça de um móvel, são gerados resíduos em diferentes tamanhos e proporções e com diferentes características [6-7]. De acordo com Hillig *et al* [8] a maioria dos resíduos gerados pela cadeia produtiva da madeira e móveis são provenientes de operações de usinagem da madeira ou da fabricação e usinagem de seus derivados.

A maior parte dos resíduos gerados é geralmente reaproveitada na própria empresa, uma vez que este reaproveitamento ocorre para a geração de energia. Uma parcela expressiva dos resíduos é vendida, enquanto que outra parte é simplesmente descartada em aterros, não agregando valor ao resíduo [9]. Assim, deve-se considerar a possibilidade de recuperação, reutilização ou reciclagem dos resíduos de madeira [10-11], os quais podem constituir matéria-prima para o desenvolvimento de compósitos a serem utilizados pela própria indústria moveleira [10-11] ou por outras indústrias buscando potencializar ainda mais a utilização de um resíduo tão nobre.

O aumento do interesse da indústria, principalmente da automotiva, na utilização de compósitos poliméricos que façam uso da biomassa vegetal vem cada vez mais proporcionando o desenvolvimento de compósitos reforçados por materiais lignocelulósicos. Estes materiais ganham espaço frente à substituição gradual das fibras inorgânicas devido ao apelo ambiental pelo desenvolvimento de materiais ambientalmente amigáveis [12-13].

Os resíduos de madeira constituem uma alternativa ao uso de fibras inorgânicas devido a baixa abrasão e baixa densidade e o que resulta em redução da densidade dos compósitos produzidos assim como reduz os gastos com manutenção dos equipamentos utilizados no processamento; nas propriedades mecânicas geralmente verifica-se aumento do módulo elástico; não são nocivas a saúde como as fibras de vidro e ainda em termos socioeconômicos e ambientais apresentam baixo custo, são amplamente disponíveis e proveniente de fontes renováveis além de serem biodegradáveis [14-17]. No entanto, os resíduos de madeira como reforço em compósitos possuem limitações como baixa adesão, absorção de umidade e baixa estabilidade térmica [18-20]. Assim, para utilizar ao máximo todo o potencial que a madeira pode oferecer como material o conhecimento de suas propriedades físicas e químicas é essencial.

Neste contexto, o presente trabalho avalia como os principais componentes da madeira e também a cristalinidade da celulose influencia na estabilidade térmica e na cinética de degradação de quatro espécies de madeiras plantadas no Brasil. Amostras das espécies *Pinus elliottii* (PIE), *Eucalyptus grandis* (EUG), originárias da Serra Gaúcha, *Mezilaurus itauba* (ITA) e *Dipteryx odorata* (DIP), provenientes da região amazônica, foram estudadas através de análises químicas, difração de raios-X, espectroscopia no infravermelho com transformada de Fourier e termogravimetria.

A presente tese é composta por uma revisão bibliográfica, seguida pelos Capítulos 1, 2 e 3 onde são apresentados na íntegra e na forma em que foram publicados os três artigos que compõem esta tese. Logo após, no Capítulo 4 uma discussão e integração dos três artigos é realizada antes das conclusões obtidas com este trabalho.

## **1.1 OBJETIVO**

### **1.1.1 Objetivo geral**

Avaliar a influência dos principais componentes da madeira na estabilidade térmica e na cinética de degradação de quatro espécies de madeira.

### **1.1.2 Objetivos específicos**

Determinar o teor de extrativos, holocelulose (celulose mais hemicelulose), lignina e teor de cinzas presentes nas espécies de madeira estudadas.

Avaliar o efeito do teor de extrativos na estabilidade térmica e na cinética de degradação das espécies de madeira estudadas.

Avaliar o efeito da cristalinidade da celulose sobre a estabilidade térmica e a cinética de degradação das espécies de madeira estudadas.

## **1.2 JUSTIFICATIVA**

O setor madeireiro brasileiro gera grandes quantidades de resíduos de madeira oriundos das indústrias de transformação da madeira. A maior parte destes resíduos é utilizada como combustível, entretanto uma parcela considerável é descartada no meio ambiente. Percebe-se a possibilidade de utilização destes resíduos no desenvolvimento de compósitos, ao invés de sua disposição no meio ambiente. Esta possibilidade não só contribui com o gerenciamento adequado dos resíduos madeireiros, como também insere novamente a madeira em novos ciclos de produção e consumo. Contudo, a necessidade de conhecer melhor as características e propriedades da madeira antes de seu uso em compósitos faz com que esta deva ser caracterizada previamente para que no momento de sua utilização a melhor combinação entre processamento, estrutura e propriedades possa ser obtida.



Pelo exposto há interesse tanto na área científica e tecnológica quanto na ambiental no reaproveitamento dos resíduos de madeira. Portanto, esta proposta fornece resultados que podem contribuir para o melhor entendimento das características e propriedades da madeira antes de seu uso em compósitos.

## 2 REVISÃO BIBLIOGRÁFICA

### 2.1 Madeira

A madeira é um material natural, portanto renovável, pode ser reaproveitada e também é biodegradável, englobando características geralmente creditadas a materiais ambientalmente amigáveis [21]. A madeira é quimicamente composta por carbono, hidrogênio e oxigênio, estruturados para formar seus três principais componentes: celulose, hemicelulose e lignina [22].

#### 2.1.1 Composição química da madeira

A madeira é um compósito natural anisotrópico formado através da organização celular da celulose, hemicelulose, lignina e em menores quantidades de extrativos e materiais inorgânicos [21,23]. A Figura 1 apresenta a representação proposta por Akerholm et al. [24] para a organização da parede celular da madeira. Nesta representação as moléculas de celulose na forma de fibrilas elementares são cercadas primeiramente pela hemicelulose para assim formar microfibrilas que por sua vez são envoltas em uma matriz de lignina.

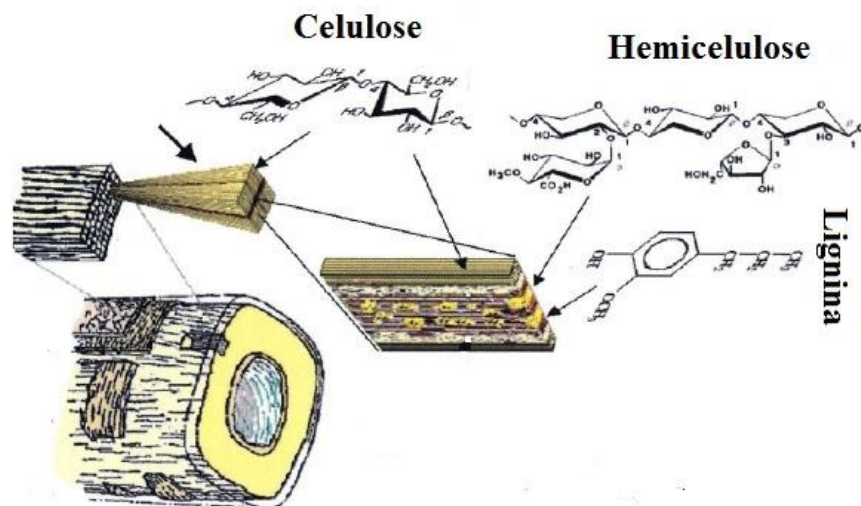


Figura 1: Estrutura celular e componentes principais da madeira [Adaptado 24].

A celulose é o componente essencial das fibras de todas as plantas [24-26]. É um polímero natural constituído por unidades repetitivas de D-

anidroglicose ( $C_6H_{11}O_5$ ) unidas por ligações glicosídicas [22, 26], conforme apresentado na Figura 2. Cada unidade repetitiva contém três grupos hidroxila conferindo a celulose alto caráter hidrofílico e suas habilidades em formar ligações hidrogênio governam as propriedades físicas bem como o empacotamento cristalino. A celulose é formada por regiões cristalinas de elevada ordenação molecular e regiões amorfas de pouca ou nenhuma ordenação. É composta por um aglomerado de microfibrilas resistentes a álcalis, mas facilmente hidrolisadas por ácidos em açúcares solúveis em água [22]. O conteúdo de celulose na madeira de coníferas geralmente varia entre 40 a 45% e na madeira de folhosas entre 38 a 49% [21].

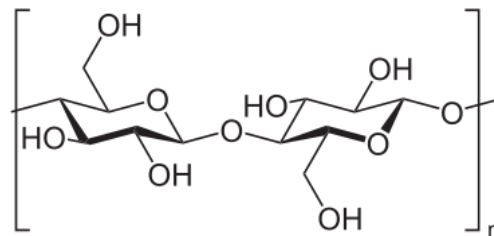


Figura 2: Estrutura química do mero da celulose [23,26].

A hemicelulose está intimamente associada à celulose e contribui para a composição estrutural da árvore. A hemicelulose é hidrofílica, solúvel em álcali e facilmente hidrolisada por ácidos [22]. O teor de hemicelulose na madeira seca oscila entre 15 e 25% [21]. A Figura 3 apresenta alguns dos compostos que fazem parte da hemicelulose.

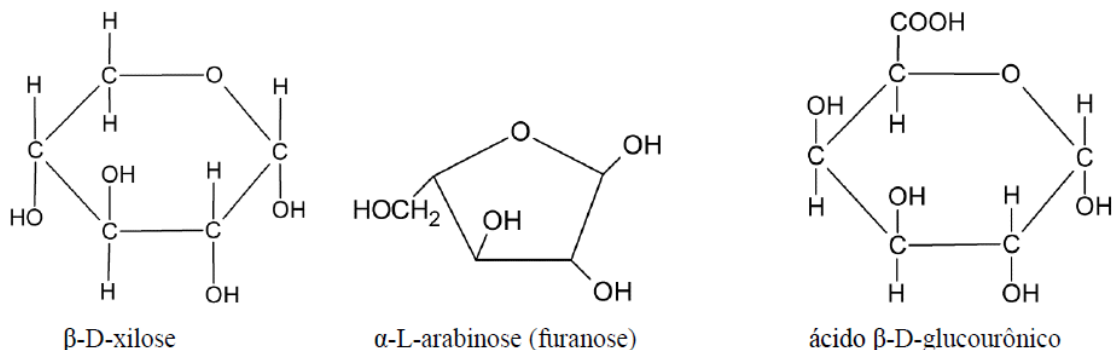


Figura 3: Alguns dos componentes da hemicelulose [21-22].

A lignina é um polímero complexo constituído por compostos alifáticos e aromáticos [22,27]. A lignina é amorfa, hidrofóbica e insolúvel em muitos solventes; é o componente que promove rigidez às plantas [22]. O conteúdo de lignina varia usualmente entre 18 e 25% para madeiras de folhosas e entre 25 e 35% para as madeiras provenientes de coníferas [21]. A Figura 4 apresenta a estrutura química da lignina proposta para uma folhosa ilustrando algumas das ligações que ocorrem entre os componentes da lignina. Algumas ligações covalentes também ocorrem entre a lignina e os demais polissacarídeos o que também aumenta a adesão entre as fibras de celulose e a matriz de lignina [28].

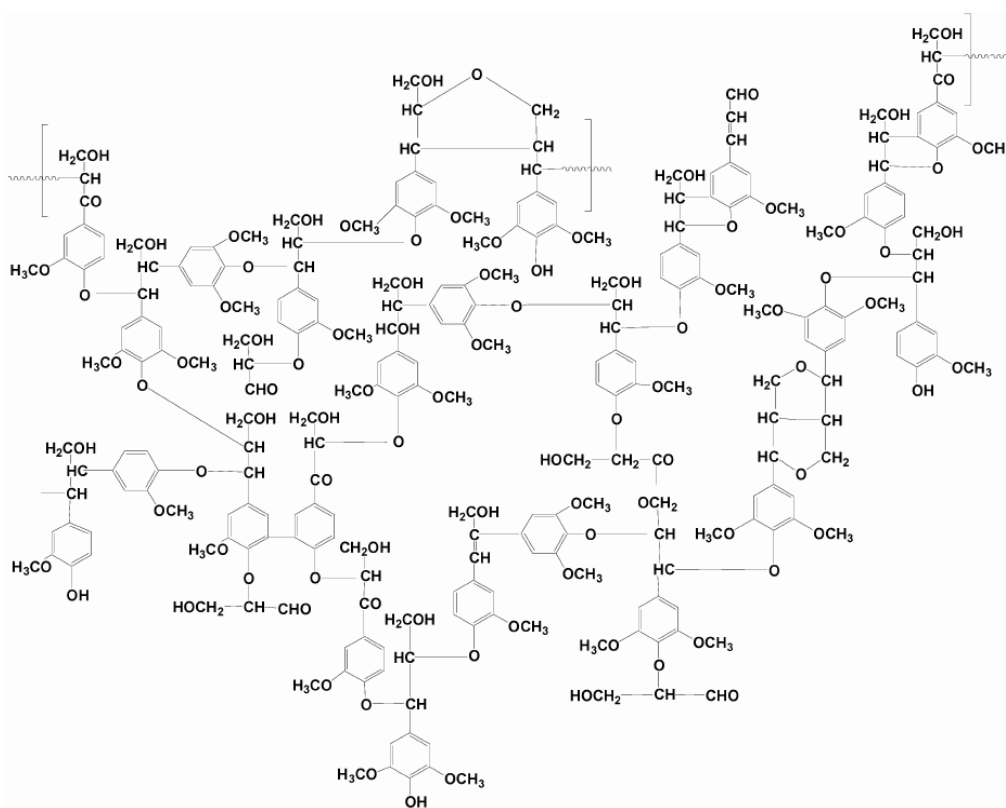


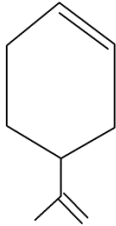
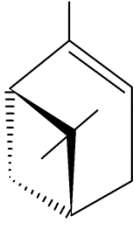
Figura 4: Modelo proposto para estrutura química da lignina [28].

Os constituintes menores incluem compostos orgânicos e compostos inorgânicos [21]. São basicamente divididos em duas classes. A primeira classe é constituída por materiais conhecidos como extrativos por serem extraídos por diversos tipos de solventes. A segunda classe engloba os compostos que não são extraídos pelos solventes, tais como compostos inorgânicos. Os constituintes menores são frequentemente responsáveis por determinadas características da planta como cor, odor e resistência natural ao

ataque de fungos [21,29]. Além disso, eles influenciam diretamente nos processos de secagem, adesão, higroscopicidade e propriedades térmicas das espécies de madeira. Aproximadamente 3 a 10% da madeira seca é constituída de extrativos [30-32]. Contudo, em algumas espécies tropicais os teores de extrativos podem chegar até 15% [33].

Os extrativos podem ser classificados em diversos grupos de acordo com sua estrutura química, como por exemplo, terpenos, flavonóides, ceras, ácidos graxos e hidrocarbonetos [29,34]. Os terpenos e seus derivados são substâncias odoríferas. As graxas são compostas por ésteres de ácidos carboxílicos de cadeias longas como o glicerol, enquanto que as ceras são ésteres de ácidos graxos com alcoóis de alta massa molecular [29,34]. A Tabela 1 apresenta alguns destes componentes.

Tabela 1: Terpenos, óleos, ceras e ácidos graxos encontrados em diversas espécies de madeira.

<b>Terpenos</b>		
	Limoneno	$\alpha$ -pineno
<b>Óleos</b>	$\begin{array}{c} \text{H}_2\text{C}-\text{O}-\text{CO}-\text{R}^1 \\   \\ \text{HC}-\text{O}-\text{CO}-\text{R}^2 \\   \\ \text{H}_2\text{C}-\text{O}-\text{CO}-\text{R}^3 \end{array}$	$\begin{array}{c} \text{H}_2\text{C}-\text{O}-\text{CO}-\text{R} \\   \\ \text{HC}-\text{OH} \\   \\ \text{H}_2\text{C}-\text{OH} \end{array}$
	Triglicerídeo	Monoglicerídeo
<b>Ceras</b>	$\text{H}_3\text{C}-\left(\text{CH}_2\right)_n-\text{O}-\text{CO}-\left(\text{CH}_2\right)_n-\text{CH}_3$	
<b>Ácidos graxos</b>	$\text{H}_3\text{C}-\left(\text{CH}_2\right)_n-\text{C}\begin{array}{l} \text{=O} \\ \text{-OH} \end{array}$	$n = 14$ Ácido hexadecanóico (palmítico) $n = 16$ Ácido octadecanóico (esteárico)

### 2.1.2 Resíduos de madeira

Os processos de usinagem da madeira são classificados em abate, descascamento, desdobro, laminação, produção de partículas e beneficiamento [5]. Cada um destes processos é constituído por operações individuais, como por exemplo, as operações de corte e lixamento, seja nas madeireiras ou nas indústrias moveleiras, geram resíduos de madeira.

O percentual de resíduos gerado em relação à quantidade de madeira processada depende, dentre outros fatores, do tipo de processo adotado, do tipo de matéria prima utilizada, das condições tecnológicas empregadas e do tipo de produto final [7]. De acordo com Hillig *et al.* [8] a maioria dos resíduos gerados pela cadeia produtiva da madeira e móveis são provenientes de operações de usinagem da madeira ou da fabricação e usinagem de seus derivados. Nas etapas de processamento da madeira, desde o abate da árvore até a operação de lixamento de qualquer peça de um móvel, são gerados resíduos em diferentes proporções e com diferentes características [11].

Estima-se que no Brasil sejam gerados 30 milhões de toneladas de resíduos de madeira anualmente [35]. A principal fonte geradora é a indústria madeireira que contribui com aproximadamente 91% do total de resíduos gerados. No entanto, pode-se afirmar que uma pequena parcela dos resíduos gerados tem algum aproveitamento econômico. A maioria dos resíduos de madeira gerados na região amazônica são simplesmente abandonados ou queimados sem nenhum fim energético o que resulta em danos ambientais e perdas econômicas significativas [35]. Por outro lado, a situação é torna-se bastante diferente quando se trata dos resíduos de madeira gerados na região sul do país. A grande maioria dos resíduos de madeira tanto da indústria madeireira quanto moveleira são aproveitados para a produção de novos produtos como painéis de madeira e celulose e também para a geração de energia. A Figura 5 apresenta um comparativo da destinação dos resíduos de madeira da região amazônica e para o polo moveleiro da Serra Gaúcha, onde torna-se evidente os contrastes quanto a melhor destinação dos resíduos na região sul do Brasil. A maior discrepância está na parcela de resíduos que é queimada. Enquanto que na Serra Gaúcha apenas 6,7% dos resíduos de madeira são queimados na região amazônica este índice atinge 35%.

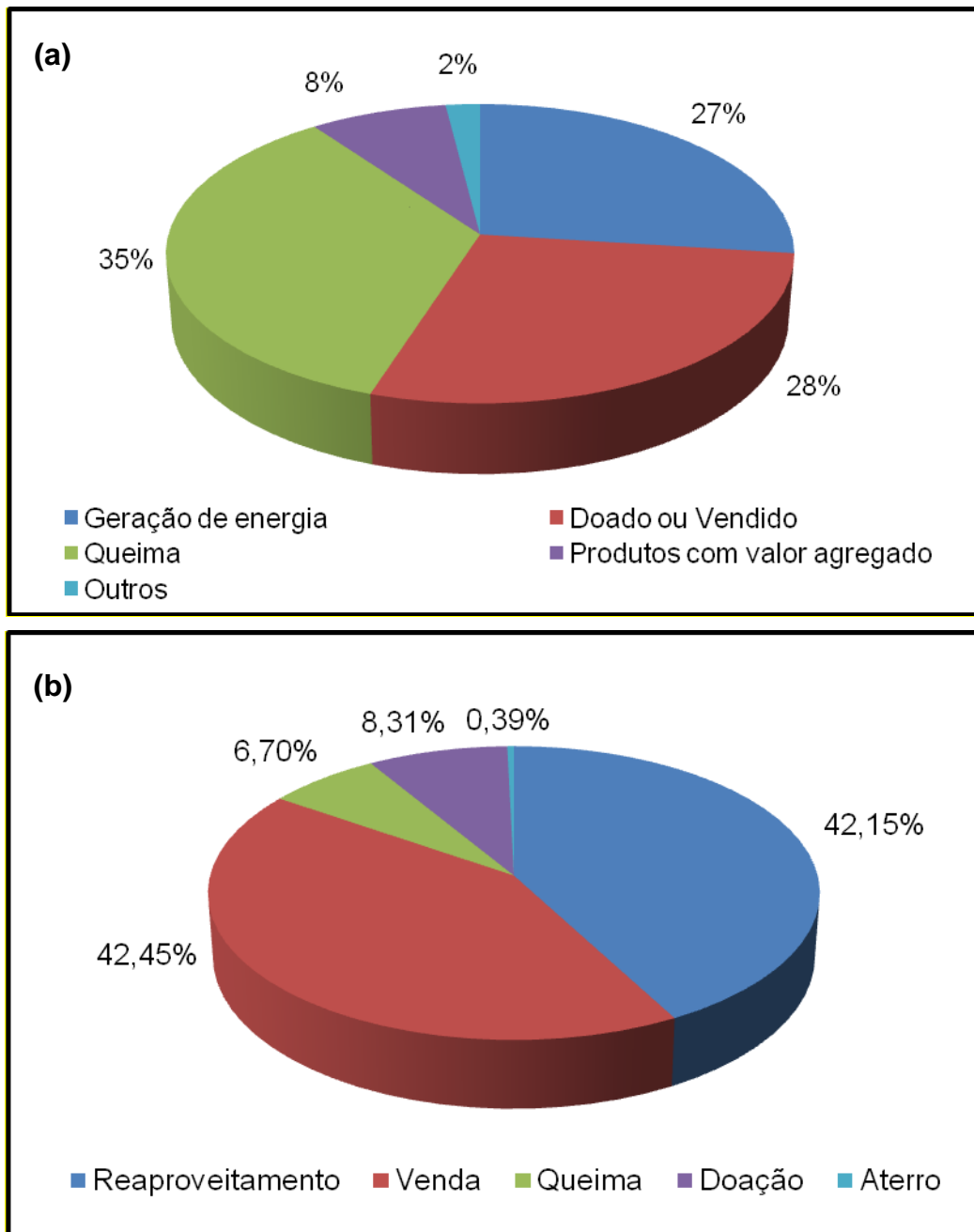


Figura 5: Destinação dos resíduos de madeira da região amazônica (a) [35] e da Serra Gaúcha (b) [9].

Deve-se considerar a possibilidade de recuperação, reutilização ou reciclagem dos resíduos de madeira, os quais podem constituir matéria-prima para o desenvolvimento de compósitos a serem utilizados pela própria indústria moveleira [9] ou por outras indústrias buscando potencializar ainda mais a utilização de um resíduo tão nobre.

## 2.2 Características da madeira e de seus componentes

Yang *et al.* [36] avaliaram a degradação térmica dos três principais componentes da madeira. Os autores observaram que a degradação da hemicelulose geralmente ocorre entre 220-315°C, enquanto que a degradação da celulose ocorre entre 315-400°C, com uma taxa máxima de perda de massa em aproximadamente 355°C. A lignina por sua vez degrada lentamente desde a temperatura ambiente até 900°C. Os autores atribuem esta diferença na estabilidade térmica dos componentes da madeira as diferenças inerentes em sua estrutura química. No entanto, conforme Popescu *et al.* [37] os componentes da madeira se comportam de forma diferente se eles estão isolados ou intimamente ligados. Os autores estudaram a degradação de diferentes espécies de madeira e verificaram que a degradação da hemicelulose inicia em torno de 170°C e estende-se até 380°C, já a degradação da lignina também inicia em 170°C e estende-se até temperaturas acima de 600°C. A degradação da celulose ocorre entre 280-400°C.

Popescu *et al.* [37-39] estudaram as características de diferentes espécies de madeira. Os autores verificaram que maiores quantidades de celulose na madeira podem ocasionar ligações hidrogênio mais intensas e assim proporcionar uma maior energia das ligações hidrogênio nas espécies de madeira com elevados teores de celulose. Os autores observaram também que a intensidade das ligações hidrogênio aumenta com o aumento da cristalinidade da celulose contida na madeira.

Shebani *et al.* [30] observaram que elevados teores de celulose e lignina na madeira associados com baixos teores de extrativos ocasionam um aumento da estabilidade térmica da madeira. Os autores verificaram também que a remoção dos extrativos da madeira ocasionou um aumento da estabilidade térmica das madeiras estudadas, uma vez que os extrativos são compostos de baixa massa molecular e que geralmente volatilizam em baixas temperaturas acelerando a degradação dos principais componentes da madeira. Guo e colaboradores [40] também observaram que madeiras com elevados teores de extrativos geralmente iniciam o processo de degradação a baixas temperaturas devido provavelmente a volatilização dos extrativos.



Em um estudo recente Tenorio e Moya [41] demonstraram que a umidade presente na madeira exerce forte influencia no processo de degradação térmica da madeira. Contudo, os autores verificaram também que outros fatores, tais como, a quantidade de extrativos, porosidade da madeira, e suas características físicas e químicas também influenciam seu processo de degradação térmica.

## **2.3 Cinética de degradação da madeira**

### **2.3.1 Energia de ativação**

Slopiecka *et al.* [42] analisaram a degradação térmica e a cinética de degradação da madeira proveniente da espécie *Populus L.* e obtiveram valores de energia de ativação variando entre 107-209 kJ/mol utilizando o método de Flynn-Wall-Ozawa (FWO) indicando que o mecanismo de degradação da madeira varia ao longo do processo de degradação e que a energia de ativação é dependente da conversão.

Poletto e colaboradores [43] estudando as madeiras provenientes das espécies de *Pinus taeda* e *Eucalyptus grandis* verificaram que quantidades elevadas de holocelulose e lignina associadas a baixos teores de extrativos aumentam a estabilidade térmica da madeira. Os valores de energia de ativação obtidos pelo método de FWO variaram entre 153-163 kJ/mol para a espécie *Pinus taeda* e entre 146-165 kJ/mol para a espécie *Eucalyptus grandis*. Segundo os autores a composição química da madeira afeta diretamente seu processo de degradação bem como sua energia de ativação. Resultados semelhantes também foram obtidos por Yao *et al.* [44] avaliando a decomposição térmica de dez tipos de fibras naturais. Os autores observaram que os valores de energia de ativação variaram entre 160-170 kJ/mol para todas as fibras estudadas.

Por outro lado, Shen *et al.* [45] analisando espécies de madeira de pinus obtiveram valores de energia de ativação variando entre 180-220 kJ/mol em um intervalo de conversão entre 10-85%. Sanchez-Silva *et al.* [46] também obtiveram valores de energia superiores a 200 kJ/mol para madeiras provenientes da espécies de pinus e eucalipto para faixas de temperatura entre

150-320°C. De acordo com Mamleev *et al.* [47] a despolimerização da celulose durante o processo de pirólise acarreta em energias de ativação da ordem de 200 kJ/mol. Carpat e colaboradores [48] também obtiveram valores de energia próximos aos obtidos por Mamleev *et al.* [47] quando avaliaram a cinética de degradação da celulose.

Kim *et al.* [49] avaliaram a decomposição térmica de três amostras de celulose. Os autores observaram que a estabilidade térmica das amostras aumenta com o aumento da cristalinidade e do tamanho dos cristalitos da celulose. Contudo, os valores de energia de ativação não são afetados por estes parâmetros.

### **2.3.2 Mecanismo de degradação**

Wang e colaboradores [50] analisando a cinética de degradação da madeira proveniente da espécie *M. glyptostriboides* verificaram que o mecanismo de degradação desta espécie ocorre através de processos de difusão nas três dimensões. Yorulmaz e Atimtay [51] observaram que amostras provenientes da espécie de pinus também mostraram mecanismos de degradação por difusão. Bianchi *et al.* [52] estudaram a degradação não isotérmica das espécies *Pinus taeda* e *Apuleia leiocarpa*. Os autores verificaram que as espécies degradam por difusão até valores de conversão de 80%, onde o mecanismo de degradação é governado por uma cinética de terceira ordem.

Ornaghi Jr. *et al.* [53] avaliaram a cinética de degradação de seis diferentes fibras vegetais. Os autores verificaram que para conversão de até 50% todas as fibras estudadas apresentaram degradação por difusão. Contudo, para valores de conversão superiores a 50% as reações de degradação por núcleos aleatórios controlaram o processo de degradação.

Dahiya *et al.* [54] estudaram a cinética de degradação da celulose e verificaram que reações de degradação por núcleos aleatórios governam o mecanismo de degradação. Poletto *et al.* [55] verificaram que amostras de celulose da espécie *Eucalyptus grandis* degradam através de mecanismo de difusão até a conversão de 40%. Contudo, para conversão superior a 50% o mecanismo tende a reações de degradação por núcleos aleatórios.

## **3 MATERIAIS E MÉTODOS**

### **3.1 Espécies de madeira**

Neste trabalho foram avaliadas quatro espécies de madeira. As espécies *Eucalyptus grandis* (EUG) e *Pinus elliottii* (PIE) provenientes da região da Serra Gaúcha e as espécies *Mezilaurus itauba* (ITA) e *Dipteryx odorata* (DIP) oriundas da Região Amazônica.

As espécies EUG e PIE foram cedidas pela empresa de móveis Madarco S/A Indústria e Comércio, situada em Caxias do Sul-RS, como resíduo de processo, proveniente de madeira de reflorestamento não tratada. Enquanto que as espécies ITA e DIP foram gentilmente fornecidas pelas madeireiras da região de Sinop-MT, também caracterizada como resíduo de madeira sem nenhum tipo de tratamento químico. O tamanho de partícula utilizado foi entre 200-300  $\mu\text{m}$ .

### **3.2 Determinação dos componentes da madeira**

Os extrativos foram removidos da madeira por meio de extração via Soxhlet em triplicata utilizando etanol/benzeno, etanol e água de acordo com a norma Tappi T204-cm-97 [56] em amostras secas em estufa a 105°C por 24h. O teor de lignina insolúvel em ácido sulfúrico também foi determinado em triplicata conforme norma Tappi T222-om-02 [57]. O teor de cinzas foi determinado através de calcinação em uma mufla a 600°C por 1h. O teor de holocelulose foi determinado por diferença.

### **3.3 Espectroscopia no infravermelho com transformada de Fourier (FTIR)**

A análise de espectroscopia no infravermelho com transformada de Fourier (FTIR – Nicolet IS10- Termo Scientific) foi obtida através da média de 32 varreduras, no intervalo de 4000  $\text{cm}^{-1}$  a 400  $\text{cm}^{-1}$ , com resolução de 4  $\text{cm}^{-1}$ . Foram confeccionadas pastilhas de KBr utilizando 5mg de amostra e 100mg de KBr, com as amostras secas em estufa a 105°C por 24h.

### **3.4 Difração de raios-X (DRX)**

Foi utilizado um difratômetro de raios X Shimadzu, modelo XRD 6000, com radiação de  $\text{CuK}\alpha$  ( $\lambda = 0,1542 \text{ nm}$ ) e passo  $0,05^\circ$ , com as amostras previamente secas em estufa a  $105^\circ\text{C}$  por 24h. A separação dos picos existentes foi realizada através da deconvolução pelo método de Gauss utilizando o software Origin.

### **3.5 Análise termogravimétrica**

As análises termogravimétricas foram realizadas em um equipamento Shimadzu TGA-50 utilizando a taxa de aquecimento de  $10^\circ\text{C}\cdot\text{min}^{-1}$ , com faixa de temperatura de  $23\text{-}800^\circ\text{C}$ , em  $\text{N}_2$  a um fluxo de  $50\text{mL}\cdot\text{min}^{-1}$ . A massa para cada amostra foi de aproximadamente 10 mg. Para a determinação da cinética de degradação das espécies de madeira foram utilizadas as taxas de aquecimento de 5, 10, 20 e  $40^\circ\text{C}\cdot\text{min}^{-1}$  com rampa de aquecimento de 23 até  $800^\circ\text{C}$ .

## 4 ARTIGOS PUBLICADOS

### 4.1 Capítulo 1 – Artigo I

# Structural Differences Between Wood Species: Evidence from Chemical Composition, FTIR Spectroscopy, and Thermogravimetric Analysis

Matheus Poletto,<sup>1,2</sup> Ademir J. Zattera,<sup>2</sup> Ruth M. C. Santana<sup>1</sup>

<sup>1</sup>Laboratory of Polymeric Materials—Engineering School, Federal University of Rio Grande do Sul -UFRGS, Porto Alegre-RS-Brazil

<sup>2</sup>Laboratory of Polymers—Center of Exact Science and Technology, University of Caxias do Sul—UCS, Caxias do Sul-RS-Brazil

Received 4 November 2011; accepted 10 February 2012

DOI 10.1002/app.36991

Published online 15 April 2012 in Wiley Online Library (wileyonlinelibrary.com).

**ABSTRACT:** In this study, the relationship between wood cellulose crystallinity, influence of extractives on wood degradation, correlation between chemical composition, and physical properties of four wood species were investigated by chemical analysis, Fourier transform infrared (FTIR) spectroscopy, and thermogravimetry. The chemical analysis showed that *Dipteryx odorata* and *Mezilaurus itauba* (ITA) contained a higher quantity of extractives and lower quantities of holocellulose and lignin than *Eucalyptus grandis* (EUG) and *Pinus elliottii*. FTIR spectroscopy indicated that higher extractives content in ITA might be associated with more intense bands at 2920,

2850, and 1510  $\text{cm}^{-1}$ . The lower values for hydrogen bond energy and hydrogen bond intensity showed that EUG contained more absorbed water than the other species. Thermogravimetry confirm that lower extractive contents leads to a better wood thermal stability. This study showed that through the methods used previous information about structure and properties of wood can be obtained before use it in composite formulations. © 2012 Wiley Periodicals, Inc. *J Appl Polym Sci* 126: E336–E343, 2012

**Key words:** wood, thermal stability; FTIR spectroscopy; thermogravimetry

## INTRODUCTION

Wood is a natural composite consisting of cellulose, hemicellulose, and lignin, along with smaller quantities of extractives. Cellulose is a linear polymer of glucose units which can form intrachain and interchain bonds yielding a crystalline macromolecule<sup>1</sup> with higher molecular weight than the other wood components. The hydroxyl groups and their ability to form hydrogen bonds play a major role in directing the crystalline packing and also govern the physical properties of cellulose.<sup>1</sup> Hemicelluloses comprise a group of polysaccharides composed of a combination of 5- and 6-carbon ring sugars.<sup>1</sup> Hemicellulose have a more irregular structure with side groups, substituent groups, and sugars present along the length of the chain.<sup>1,2</sup> Lignin is a randomized condensed polymer with many aromatic groups and is much more hydrophobic than cellulose or hemicellulose.<sup>2</sup> Wood also contains a small amount of extractives, which can include lipids, phenolic compounds,

terpenoids, fatty acids, resin acids, and waxes.<sup>3</sup> Generally, the extractives content varies between 2% and 5%, but it can be as high as 15%.<sup>4</sup>

The use of wood-based materials, such as wood flour and wood fibers, as reinforcement for thermoplastics has gained significant interest in recent years.<sup>5–9</sup> Wood offers a number of advantages over conventional reinforcing materials such as abundance, renewability, low-specific gravity, high-specific strength, and stiffness, and relatively low cost.<sup>10</sup> On the other hand, there are some drawbacks, such as a high level of moisture absorption, relatively low degradation temperatures around 200°C, and filler agglomeration because of the tendency of wood to form hydrogen bonds.<sup>5,11</sup> However, the relationship between the structural parameters, such as wood cellulose crystallinity, the influence of extractives content on wood degradation, and the correlation between the chemical composition and physical properties of wood are aspects that have not been fully explored. In order to better understand such relationships, the aim of this article was to establish the main structural differences between wood samples of different species through chemical analysis, Fourier transform infrared (FTIR) spectroscopy, and thermogravimetry analysis.

Correspondence to: M. Poletto (mpolett1@ucs.br).

Contract grant sponsor: CAPES.

TABLE I  
Chemical Compositions of Wood Samples of the Species Investigated

Wood species	Holocellulose (%)	Lignin (%)	Extractives (%)	Ash (%)
<i>Eucalyptus grandis</i> (EUG)	62.7 ± 1.4	32.1 ± 1.0	4.1 ± 0.2	1.1 ± 0.3
<i>Pinus elliottii</i> (PIE)	61.2 ± 1.1	33.8 ± 1.0	4.5 ± 0.1	0.8 ± 0.1
<i>Dipteryx odorata</i> (DIP)	57.1 ± 0.6	30.4 ± 0.4	11.1 ± 0.1	1.5 ± 0.2
<i>Mezilaurus itauba</i> (ITA)	57.8 ± 1.0	28.0 ± 0.3	13.6 ± 0.7	0.7 ± 0.1

## EXPERIMENTAL

### Materials

The wood flour samples used in this study were obtained from wastes of the lumber industry in Brazil. The species investigated were *Pinus elliottii* (PIE), *Eucalyptus grandis* (EUG), *Mezilaurus itauba* (ITA), and *Dipteryx odorata* (DIP). The samples were dried at 105°C for 24 h in a vacuum oven before the tests. The average fiber particle length of the wood samples was around 200 μm.

### Determination of wood components

Benzene and absolute ethanol, purchased from Vetec Chemical (Rio de Janeiro, Brazil), were used to determine the amount of organic extractives in the wood samples. Sulfuric acid, purchased from Vetec Chemical, was used for insoluble lignin determination. The wood extractives were eliminated from the samples via Soxhlet extraction in triplicate using: ethanol/benzene, ethanol, and hot water, according to the Tappi T204 cm-97 standard. The Klason lignin content was determined according to the Tappi T222 om-02 standard. The ash content was determined by calcination in a muffle furnace at 600°C for 1 h. The holocellulose content (cellulose + hemicellulose) was determined according to eq. (1)<sup>12</sup>:

$$\% \text{Holocellulose} = 100 - (\% \text{Lignin} + \% \text{Extractives} + \% \text{Ash}) \quad (1)$$

### Fourier transform infrared (FTIR) spectroscopy

FTIR spectra were obtained on a Nicolet IS10-Thermo Scientific spectrometer. Wood powder samples of each species (5 mg) were dispersed in a matrix of KBr (100 mg), followed by compression to form pellets. The spectra were obtained using 32 scans, in the range of 4000 cm<sup>-1</sup> to 400 cm<sup>-1</sup>, at a resolution of 4 cm<sup>-1</sup>. The magnitude FTIR spectra were normalized at 1435 cm<sup>-1</sup>.<sup>13</sup> Second derivative spectra were obtained by applying the Savitzky-Golay function.

### Thermogravimetric analysis

The thermogravimetric analysis (TGA50—Shimadzu) was carried out under constant nitrogen flow (50

mL/min), from 25 to 600°C, at a heating rate of 10°C/min. Approximately 10 mg of each sample was used.

## RESULTS AND DISCUSSION

### Wood components

The chemical compositions of the wood samples of the different species studied are showed in Table I. The holocellulose content was determined to be around 63% for EUG, 61% for PIE, and 57% for both DIP and ITA. However, ITA and DIP contain three times more extractives than EUG and PIE. The degradation temperature of a wood sample is expected to be related to the heat stability of the individual wood components.<sup>3,14</sup> Thus, differences in the thermal stability of wood samples from different species can be attributed to variations in the chemical composition and structure of the wood components.<sup>15</sup> The PIE had the highest lignin content with around 34% while ITA had the lowest at 28%. The ash content was quite similar for all wood samples studied.

The wood samples of the four species investigated have clearly distinguishable differences in their composition and differences in the structure of the wood components and the thermal behavior can therefore be expected.

### FTIR spectroscopy

FTIR spectroscopy has been used as a simple technique for obtaining rapid information on the structure of wood constituents and chemical changes taking place in wood due to various treatments.<sup>16,17</sup> In contrast to conventional chemical analysis, this method requires small sample sizes, short analysis time, and does not destroy the wood structure.<sup>2</sup>

Because of their complexity, the spectra were separated into two regions, namely: the OH and CH stretching vibrations in the 3800–2700 cm<sup>-1</sup> region (Fig. 1) and the “fingerprint” region which is assigned to stretching vibrations of different groups of wood components at 1800–800 cm<sup>-1</sup> (Fig. 3). The FTIR spectra and second derivative spectra for the different wood samples studied in the region of 3800–2700 cm<sup>-1</sup> are shown in Figure 1(a,b), respectively. It can be observed in Figure 1(a) that there is a strong broad band at around 3400 cm<sup>-1</sup> which is



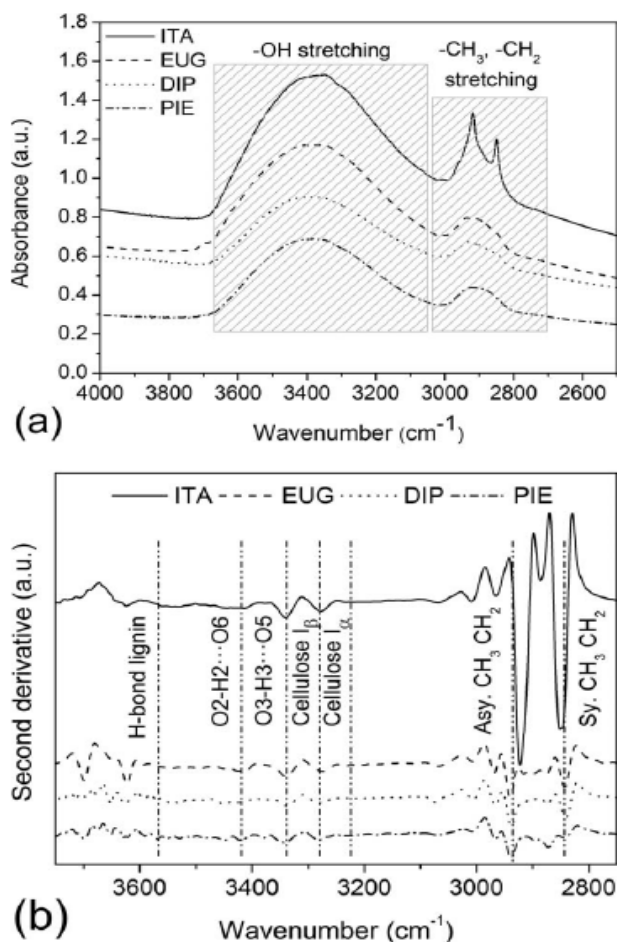


**Figure 1** FTIR spectra (a) and the second derivative spectra (b) of the wood samples studied O(2)H-O(6)(intra), O(3)H-O(5) (intra), O(6)H-O(3')(inter).

assigned to different O—H stretching modes and another two bands at around 2920 and 2850  $\text{cm}^{-1}$  related to asymmetric and symmetric methyl and methylene stretching groups present in the spectra of all of the wood components but most notably in the spectra for cellulose,<sup>18,19</sup> shown in detail in Figure 1(b). However, these two bands are more prominent in the ITA spectra at 2916 and 2852  $\text{cm}^{-1}$ , respectively. This might be attributed to the higher extractives content in this wood, since some compounds in organic extractives, like fatty acid methyl esters and phenolic acid methyl esters, contain methyl and methylene groups.<sup>20–22</sup>

According to the literature,<sup>2,23</sup> there are intermolecular and intramolecular H-bonds in cellulose I and in lignin. In cellulose I a secondary OH group at the C3 position forms an H-bond with an O5 atom of the adjacent ring (O3—H3...O5 intramolecular H-bond), and another secondary OH group at the C2 position forms an H-bond with an O6 atom

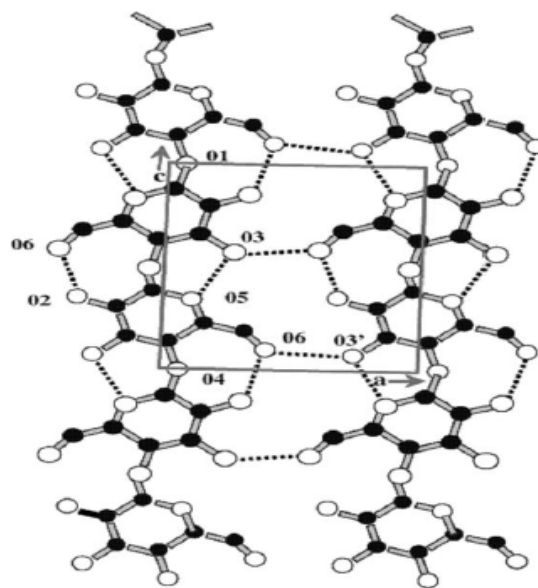
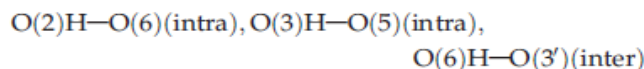


**Figure 2** Proposed hydrogen-bonding in cellulose I/cellulose II by Kolpak and Blackwell (Oh et al.,<sup>23</sup>).

of the adjacent ring (O2—H2...O6 intramolecular H-bond). A primary OH group in the C6 position is involved in an H-bond with an O3 atom in the neighboring chain (O6—H6...O3' intermolecular H-bond), as can be seen in Figure 2. Also, aliphatic hydroxyl groups in lignin have the potential to form stronger intermolecular hydrogen bonds than phenolic hydroxyl groups.



The hydroxyl stretching region is particularly useful for elucidating hydrogen-bonding patterns. However, the bands described below can generally be seen only in the second derivative of the FTIR spectra, which normally enhance the apparent resolution and amplify small differences in the FTIR spectrum.<sup>2</sup> Figure 1(b) shows the main bands in this region. Each distinct hydroxyl group in this region gives a single stretching band at a frequency that decreases with increasing strength of the hydrogen-bonding. These H-bonds are considered to be responsible for various properties of native cellulose, lignin, and, of course, wood itself.<sup>2,23</sup> Thus, the closer the cellulose chains the greater the interaction between the adjacent chains, resulting in more and stronger H-bonds which can lead to greater packing of cellulose chains and an increase in the strength of wood.

The intramolecular hydrogen bond in a phenolic group in lignin is observed at around 3568–3577  $\text{cm}^{-1}$ .<sup>17</sup> In cellulose, an intramolecular hydrogen

TABLE II  
The Energy of the Hydrogen Bonds and Hydrogen Bond Distance for Wood Samples Studied

Wood species	3567 cm <sup>-1</sup>		3423 cm <sup>-1</sup>		3342 cm <sup>-1</sup>		3278 cm <sup>-1</sup>		3221 cm <sup>-1</sup>	
	E <sub>H</sub> (kJ)	R (Å)	E <sub>H</sub> (kJ)	R (Å)	E <sub>H</sub> (kJ)	R (Å)	E <sub>H</sub> (kJ)	R (Å)	E <sub>H</sub> (kJ)	R (Å)
<i>Eucalyptus grandis</i> (EUG)	6.185	2.832	16.182	2.800	22.438	2.782	26.574	2.768	30.349	2.756
<i>Pinus elliottii</i> (PIE)	6.329	2.831	16.757	2.799	22.007	2.782	26.394	2.768	30.314	2.757
<i>Dipteryx odorata</i> (DIP)	6.401	2.831	16.613	2.799	22.438	2.781	26.610	2.768	30.874	2.754
<i>Mezilaurus itauba</i> (ITA)	6.473	2.831	16.325	2.800	22.295	2.781	26.753	2.767	30.493	2.756

bond vibration, derived from O2—H2...O6, appears at around 3432 cm<sup>-1</sup>.<sup>23,24</sup> The frequencies for the O3—H3...O5 intramolecular hydrogen bond in cellulose normally occur at 3342 cm<sup>-1</sup>.<sup>24</sup> The two characteristic bands assigned to the two crystalline cellulose allomorphs, cellulose I<sub>α</sub> and cellulose I<sub>β</sub>, also occur in the region of 3220–3280 cm<sup>-1</sup>.<sup>2</sup> A very small peak, normally shifted to lower wavenumbers, at 3221 cm<sup>-1</sup> was attributed to hydrogen bonds only in cellulose I<sub>α</sub>.<sup>2,23</sup> The band at 3221 cm<sup>-1</sup> is assigned to the O6—H6...O3 intramolecular hydrogen bonds present only in triclinic I<sub>α</sub> cellulose, whereas the band at close to 3277 cm<sup>-1</sup> is proportional to the amount of monoclinic cellulose I<sub>β</sub>.

The energy of the hydrogen bonds E<sub>H</sub> for several OH stretching bands has been calculated using eq. (2):<sup>25</sup>

$$E_H = \frac{1}{k} \left[ \frac{(v_o - v)}{v_o} \right] \quad (2)$$

where v<sub>o</sub> is the standard frequency corresponding to free OH groups (3650 cm<sup>-1</sup>), v is the frequency of the bonded OH groups, and k is a constant (1/k = 2.625 × 10<sup>2</sup> kJ).

The energy of hydrogen bonds are presented in Table II where it can be observed that they are very similar; however, the energy of the hydrogen bond for EUG at 3567 cm<sup>-1</sup> shows a small decrease when compared with the other species. This could be associated with a higher quantity of absorbed water in the structure of EUG, since the band at 3567 cm<sup>-1</sup> is assigned to the weakly absorbed water in free OH(6) and OH(2).<sup>24,26,27</sup>

The hydrogen bond distances R are obtained using the Pimentel and Sederholm equation as follows<sup>28</sup>:

$$\Delta v(\text{cm}^{-1}) = 4430 \times (2.84 - R) \quad (3)$$

where Δv = v<sub>o</sub> - v, v<sub>o</sub> is the monomeric OH stretching frequency, which is taken to be 3600 cm<sup>-1</sup>, and v is the stretching frequency observed in the infrared spectrum of the sample. The hydrogen bond distances of the samples are quite similar for the species studied at all wavenumbers considered, as can be seen in Table II. Also, these values are close to that obtained by Popescu et al.<sup>18</sup>

In the "fingerprint" region, the spectra contain several bands assigned to the main wood components, as can be seen in Figure 3. The bands at 1595, 1510, and 1270 cm<sup>-1</sup> are assigned to C=C, C—O stretching or bending vibrations of different groups present in lignin. The bands at 1460, 1425, 1335, 1220, and 1110 cm<sup>-1</sup> are characteristic of C—H, C—O deformation, bending, or stretching vibrations of many groups in lignin and carbohydrates. The bands at 1735, 1375, 1240, 1165, 1060, 1030 cm<sup>-1</sup> are assigned to C=O, C—H, C—O—C, C—O deformation or stretching vibrations of different groups in carbohydrates.<sup>18,26</sup>

The band at 1735 cm<sup>-1</sup> is assigned to C=O stretching vibrations of the carboxyl and acetyl groups in hemicellulose.<sup>18,26</sup> Higher holocellulose content is indicated by a strong and broad band at 1735 cm<sup>-1</sup>.<sup>29</sup> The EUG shows a more prominent band than the other three wood at 1736 cm<sup>-1</sup>, in agreement with the highest content of holocellulose observed for this species, see Table I. The absorption peak at 1510 cm<sup>-1</sup> arising from the aromatic skeletal vibration C=C of the benzene ring is characteristic of lignin.<sup>26,29</sup> For this band, the ITA and DIP species presented the most prominent band indicating higher lignin content than the EUG and PIE species,

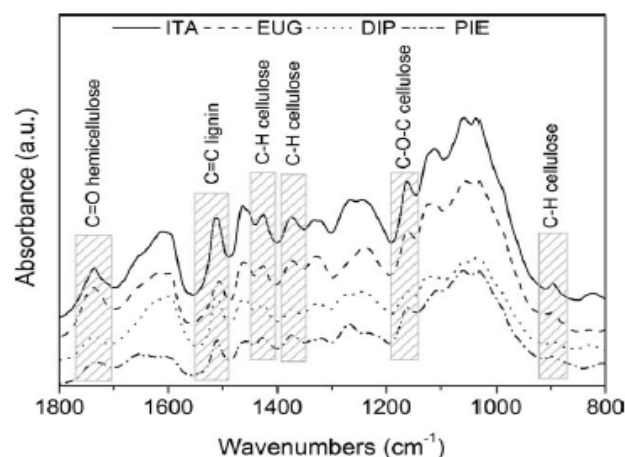


Figure 3 FTIR spectra in the 1800–800 cm<sup>-1</sup> region.



according to Figure 3. However, the chemical method used to determine the wood components presented in Table I revealed that EUG and PIE contain more lignin than ITA and DIP. A probable explanation for this fact is that ITA and DIP contain around three times more extractives than EUG and PIE and some compounds of the extractives might be absorbed at around  $1510\text{ cm}^{-1}$ . An example of this is the benzoic acids presents in wood tannins<sup>20</sup> that contain aromatic rings in their structure, and since the absorption at  $1510\text{ cm}^{-1}$  is assigned to C=C stretching of the aromatic ring this may influence the intensity of this band. Pandey (2005)<sup>30</sup> observed in wood samples which contain a much higher amount of organic extractives that these compounds have a significant contribution to the  $1510\text{ cm}^{-1}$  peak. Therefore, great care needs to be taken when using the peak at  $1510\text{ cm}^{-1}$  to compare the different lignin contents and lignin/carbohydrate ratios in wood samples from species with higher contents of extractives.

The band at  $1420\text{--}1430\text{ cm}^{-1}$  is related to aromatic skeletal vibrations associated with C-H in plane deformation of cellulose.<sup>31</sup> The bands at  $1372\text{ cm}^{-1}$  and  $1160\text{ cm}^{-1}$  are bands characteristic of carbohydrates. The band at  $1375\text{ cm}^{-1}$  is assigned to CH bending in cellulose and hemicellulose while the band at  $1165\text{ cm}^{-1}$  is assigned to C-O-C asymmetric stretching vibrations in cellulose and hemicellulose.<sup>13</sup> The band at  $898\text{ cm}^{-1}$  is assigned to CH deformation in cellulose.<sup>13,23</sup> The band at around  $1420\text{--}1430\text{ cm}^{-1}$  is designated as associated with the amount of crystalline structure of the cellulose, while the band at  $898\text{ cm}^{-1}$  is assigned to the amorphous region in cellulose.<sup>13</sup> The ratio between the two bands was defined as an empirical crystallinity index proposed by Nelson and O'Connor (1964)<sup>32</sup> as a lateral order index (LOI). The ratio between the bands at  $1372\text{ cm}^{-1}$  and  $2900\text{ cm}^{-1}$ , proposed by Nelson and O'Connor (1964)<sup>32</sup> to be the total crystalline index (TCI), was used to evaluate the infrared crystallinity (IR) ratio. Considering the chain mobility and bond distance, the hydrogen bond intensity (HBI) of cellulose is closely related to the crystal system and the degree of intermolecular regularity, that is, crystallinity, as well as the amount of bound water.<sup>31</sup> The ratio between the absorbance bands at  $3400$  and  $1320\text{ cm}^{-1}$  was used to study the HBI of the wood samples of the different species. The band at  $1320\text{ cm}^{-1}$  is assigned to the  $\text{CH}_2$  rocking vibration in cellulose.<sup>26</sup> The results obtained are presented in Table III.

The TCI is proportional to the degree of crystallinity of cellulose.<sup>33</sup> in wood and the LOI is correlated to the overall degree of order in the cellulose.<sup>33,34</sup> EUG showed the highest TCI and LOI values indicating the highest degree of crystallinity and a more

TABLE III  
Infrared Crystallinity Ratio and Hydrogen Bond Intensity for the Wood Sample

Wood species	IR crystallinity ratio		HBI
	H1372/ H2900 (TCI)	H1429/ H897 (LOI)	A3400/ A1320
<i>Eucalyptus grandis</i> (EUG)	0.608	3.172	1.440
<i>Pinus elliottii</i> (PIE)	0.474	2.299	1.598
<i>Dipteryx odorata</i> (DIP)	0.389	3.137	1.508
<i>Mezilaurus itauba</i> (ITA)	0.237	2.060	1.523

ordered cellulose structure than the other species. On the other hand, ITA presented the lowest TCI and LOI values which may indicate that the cellulose of this wood is composed of more amorphous domains when compared with the other three species evaluated, while PIE and DIP presented intermediate values. Another interesting finding is that DIP presented a high LOI value, similar to that of EUG, which is associated with a lateral ordered cellulose structure. The crystallinity of the cellulose in wood is closely related to the thermal stability of the wood.<sup>35,36</sup> Therefore, it is possible that wood samples with higher TCI and LOI values have a greater thermal stability. However, EUG had the lowest HBI value. This result may be associated with a greater amount of absorbed water in the EUG wood, since the HBI value also represents the amount of absorbed water.<sup>31</sup> This is in agreement with EUG having the lowest value for the hydrogen bond energy at  $3567\text{ cm}^{-1}$  which is assigned to the weakly absorbed water on free OH(6) and OH(2),<sup>24,26,27</sup> see Table II. The PIE sample had the highest HBI value while DIP and ITA presented similar values.

#### Thermogravimetric analysis

The thermal stability of wood flour used as a filler or reinforcement in polymer matrix composites is of paramount importance.<sup>14,37</sup> The manufacturing of composites requires the mixing of lignocellulosic materials and the polymer matrix at temperatures of around  $200^\circ\text{C}$  for the most common thermoplastic polymers.<sup>11,37</sup> The degradation of wood due to high temperatures at the time of processing may lead to undesirable properties, such as odor and browning, along with a reduction in mechanical properties.<sup>3,14</sup> Hence, it is imperative that the degradation profile of wood flour is determined prior to its use in composite applications.<sup>37</sup> The thermal analysis curves for the wood samples of the four different species studied are presented in Figure 4.

Figure 4(a) gives the weight loss as a function of temperature, while Figure 4(b) presents the derivative thermogravimetric curves. All curves show a

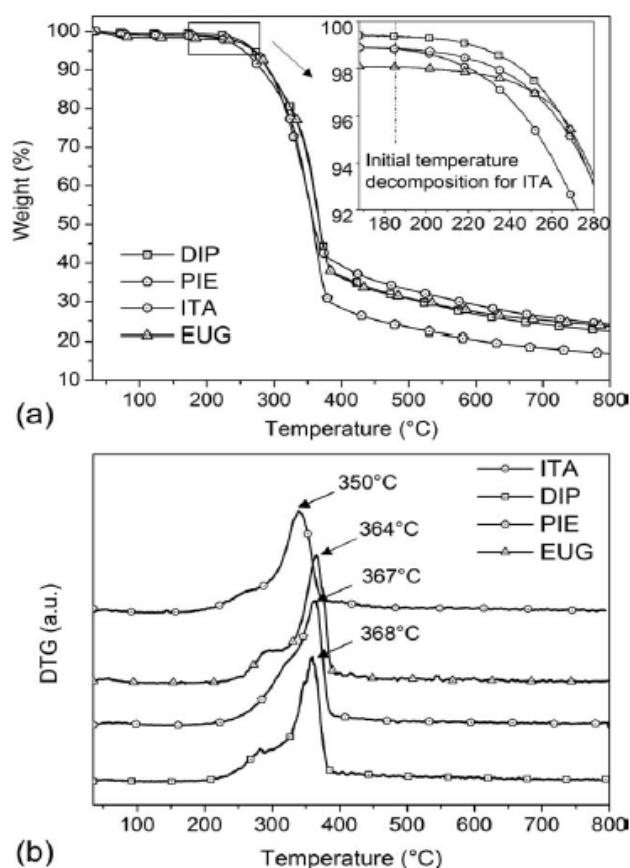


**Figure 4** TGA (a) and DTG (b) curves for the wood species studied.

small weight loss below 100°C, which can be attributed to the evaporation of water. After this small weight loss, the degradation process occurs as a two-step process. In the first step, the degradation of hemicellulose takes place at around 300°C and a slight shoulder in the DTG curve can be seen in Figure 4(b) for all wood species studied. At around 350–370°C the main degradation of cellulose occurs and a prominent peak appears at the temperature corresponding to the maximum decomposition rate. According to Kim et al. (2006),<sup>38</sup> the depolymerization of hemicellulose occurs between 180 and 350°C, the random cleavage of the glycosidic linkage of cellulose between 275 and 350°C, and the degradation of lignin between 250 and 500°C.

As can be seen in detail in Figure 4(a), at temperatures around 180°C the ITA wood shows a more significant weight loss. This behavior might be associated with the highest content of extractives being found in this wood, around 14%, as seen in Table I. Extractives are compounds with lower molecular mass, when compared to cellulose, that can promote ignition of the wood at lower temperatures as a

result of their higher volatility and thus accelerate the degradation process. Thus, the degradation of one wood component may accelerate the degradation of the others. However, the wood of DIP, which contains around 11% of extractives, showed higher thermal stability than ITA. This behavior may be related to the higher content of lignin in DIP than in ITA.

Wood is commonly used as filler in polymers processed at temperatures around 200°C.<sup>3,11</sup> Accounting to this fact, ITA and PIE woods initiate a more pronounced degradation process at around 180–190°C and 190–200°C, respectively. The low degradation temperature of ITA and PIE samples can lead to undesirable composite properties when processed at temperatures above 200°C. On the other hand, DIP and EUG woods initiate a more pronounced degradation process at around 220°C which can lead to thermoplastic polymer composites with higher mechanical and thermal properties by increasing the processing temperature range.

The EUG presented a slightly more pronounced weight loss at lower temperatures, around 2% at 100°C. This finding may be associated with the absorbed water in the EUG wood structure, corroborating the lower values for the hydrogen bond energy at 3567 cm<sup>-1</sup> and hydrogen intensity, see Tables II and III. However, due to the high content of holocellulose and lignin, the most pronounced weight loss of the EUG wood starts at around the same temperature as that for the PIE wood, as can be seen in detail in Figure 4(a).

The initial weight loss temperature,  $T_i$ , of all samples, considered as the temperature at which the sample loses 3% of its weight, as shown in Table IV. ITA presented the lowest  $T_i$  value, as can be seen in detail in Figure 4(a). This may be associated with higher volatility of extractives and hemicellulose in this wood. The highest  $T_i$  values were observed for the EUG, PIE, and DIP wood species. On the other hand, EUG, ITA, and DIP had a significant amount of residue at 800°C probably due to higher inorganic contents in these three wood species.

All samples showed a shoulder at around 300°C associated with the main degradation of hemicellulose.<sup>39</sup> This shoulder is better evinced for the ITA,

**TABLE IV**  
Thermal Degradation Temperatures and Residue at 800°C for the Wood Species Studied

Wood species	$T_i$ (°C) 3 wt % loss	$T$ shoulder (°C)	DTG peak (°C)	Residue at 800°C (%)
<i>Eucalyptus grandis</i> (EUG)	250	291	364	23.6
<i>Pinus elliottii</i> (PIE)	251	322	367	16.8
<i>Dipteryx odorata</i> (DIP)	257	289	368	22.4
<i>Mezilaurus itauba</i> (ITA)	237	275	350	24.1



EUG, and DIP wood species, as can be seen in Figure 4(b). For PIE the shoulder occurs at a higher temperature than for the other wood species. This result may be a consequence of lower extractives volatility and lower hemicellulose reactivity. The main degradation of cellulose occurs at higher temperatures for EUG, PIE, and DIP respectively. For EUG the main degradation temperature of cellulose occurs at 364°C and might be related to the higher content of holocellulose and lower content of extractives in this wood, see Table I. For ITA wood the main degradation of cellulose occurs at 350°C, around 14°C lower than the EUG wood, in agreement with the degradation of one component with lower molecular weight, such as the extractives, may accelerate the degradation process of the other wood components, such as the cellulose. This confirms the higher crystallinity of the cellulose in EUG when compared to ITA, indicated by the highest TCI and LOI values observed for EUG in Table III, which increases the thermal stability of wood.

The amount of DIP extractives is higher while the content of holocellulose is lower than those of EUG and PIE. However, the thermal stability was more pronounced and the main decomposition of cellulose was higher for DIP as compared to EUG and PIE. This behavior may be associated with the highest LOI of cellulose in this wood. The more ordered cellulose chains in this wood species may be caused by higher thermal stability.

Wood is an anisotropic material and its decomposition is a complex process. It may be difficult to distinguish and model the thermal decomposition behavior of each specific component in wood due to the complexity of growth of wood which causes variance in components content, crystal structure, and chemical composition from one species to another.<sup>14,39,40</sup>

## CONCLUSIONS

In conclusion, the three methods used to characterize wood samples of four different species were found to be appropriate to evaluate differences in the structures of wood components. The chemical analysis revealed that the wood samples of the DIP and ITA species contain a higher quantity of extractives and a lower quantity of holocellulose and lignin than EUG and PIE. In the FTIR spectroscopy analysis, it was observed that the higher extractives content in ITA wood might be associated with the prominent bands at 2920, 2850, and 1510  $\text{cm}^{-1}$ , indicating that care needs to be taken when using these bands to compare the different lignin contents and lignin/carbohydrate ratios of wood samples with higher extractives contents. The lower values for the hydrogen bond energy at 3567  $\text{cm}^{-1}$  and hydrogen

intensity indicate that the EUG wood contained more absorbed water than the samples of the other species and the thermogravimetric analysis confirmed this result. The thermogravimetric results confirmed that higher quantities of holocellulose, higher crystallinity, a more ordered cellulose structure, and higher quantities of lignin associated with a lower content of extractives lead to wood with a better thermal stability.

The authors acknowledge Prof. Ricardo Campomanes for supplying the wood samples of *Mezilaurus itauba* and *Dipteryx odorata*.

## References

- John, M. J.; Thomas, S. *Carbohydr Polym* 2008, 71, 343.
- Popescu, M.-C.; Popescu, C.-M.; Lisa, G.; Sakata, Y. *J Mol Struct* 2011, 988, 65.
- Shebani, A. N.; van Reenen, A. J.; Meincken, M. *Thermochim Acta* 2008, 481, 52.
- Zhang, X.; Nguyen, D.; Paice, M.; Tsang, A.; Renaud, S. *Enzyme Microb Technol* 2007, 40, 866.
- Nachtigall, S. M. B.; Cerveira, G. S.; Rosa, S. M. L. *Polym Test* 2007, 26, 619.
- Adhikary, K. B.; Pang, S.; Staiger, M. P. *Compos B* 2008, 39, 807.
- Kim, J.-W.; Harper, D. P.; Taylor, A. M. *J Appl Polym Sci* 2009, 112, 1378.
- Ashori, A.; Nourbakhsh, A. *Bioresour Technol* 2010, 101, 2515.
- Poletto, M.; Dettenborn, J.; Zeni, M.; Zattera, A. *J Waste Manage* 2011, 31, 779.
- Bengtsson, M.; Le Bailly, M.; Oksman, K. *Compos A* 2007, 38, 1922.
- Araújo, J. R.; Waldman, W. R.; De Paoli, M. A. *Polym Degrad Stab* 2008, 93, 1770.
- Rowell, R. *Handbook of Wood Chemistry and Wood Composites*; CRC Press: Boca Raton, 2005.
- Åkerholm, M.; Hinterstoisser, B.; Salmén, L. *Carbohydr Res* 2004, 339, 2889.
- Poletto, M.; Dettenborn, J.; Pistor, V.; Zeni, M.; Zattera, A. *J Mater Res* 2010, 13, 375.
- Marcovich, N. E.; Reboledo, M. M.; Aranguren, M. I. *Thermochim Acta* 2001, 372, 45.
- Chen, H.; Ferrari, C.; Yao, J.; Raspi, C.; Bramanti, E. *Carbohydr Polym* 2010, 82, 772.
- Popescu, C.-M.; Popescu, M.-C.; Vasile, C. *Carbohydr Polym* 2010, 82, 362.
- Popescu, C.-M.; Singurel, G.; Popescu, M.-C.; Vasile, C.; Argyropoulos, D. S.; Wilför, S. *Carbohydr Polym* 2009, 77, 851.
- Adel, M. A.; Abb El-Wahab, Z. H.; Ibrahim, A. A.; Al-Shemy, M. T. *Carbohydr Polym* 2011, 83, 676.
- Yokoi, H.; Nakase, T.; Goto, K.; Ishida, Y.; Ohtani, H.; Tsuge, S.; Sonoda, T.; Ona, T. *J Anal Appl Pyrolysis* 2003, 67, 191.
- Ishida, Y.; Goto, K.; Yokoi, H.; Tsuge, S.; Ohtani, H.; Sonoda, T.; Ona, T. *J Anal Appl Pyrolysis* 2007, 78, 200.
- Mészáros, E.; Jakab, E.; Várhegyi, G. *J Anal Appl Pyrolysis* 2007, 98, 61.
- Oh, S. Y.; Yoo, D. I.; Shin, Y.; Kim, H. C.; Kim, H. Y.; Chung, Y. S.; Park, W. H.; Youk, J. H. *Carbohydr Res* 2005, 340, 2376.
- Kondo, T. *Cellulose* 1997, 4, 281.
- Struszczyk, H. *J Mol Sci A* 1986, 23, 973.
- Schwanninger, M.; Rodrigues, J. C.; Pereira, H.; Hinterstoisser, B. *Vib Spectrosc* 2004, 36, 23.

27. Popescu, C.-M.; Popescu, M.-C.; Singurel, G.; Vasile, C.; Argyropoulos, D. S.; Willför, S. *Appl Spectrosc* 2007, 61, 1168.
28. Pimentel, G. C.; Sederholm, C. H. *J Chem Phys* 1956, 24, 639.
29. Pandey, K. K. *J Appl Polym Sci* 1999, 71, 1969.
30. Pandey, K. K. *Polym Degrad Stab* 2005, 87, 375.
31. Oh, S. Y.; Yoo, D. I.; Shin, Y.; Seo, G. *Carbohydr Res* 2005, 340, 417.
32. Nelson, M. L.; O'Connor, R. T. *J Appl Polym Sci* 1964, 71, 1311.
33. Carrilo, F.; Colom, X.; Suñol, J. J.; Saunina, J. *Eur Polym J* 2004, 40, 2229.
34. Corgié, S. C.; Smith, H. M.; Walker, L. P. *Biotechnol Bioeng* 2011, 108, 1509.
35. Kim, U.-J.; Eom, S. H.; Wada, M. *Polym Degrad Stab* 2010, 95, 778.
36. Poletto, M.; Pistor, V.; Zeni, M.; Zattera, A. J. *Polym Degrad Stab* 2011, 96, 679.
37. Tserki, V.; Matzinos, P.; Kokkou, S.; Panayiotou, C. *Compos A* 2005, 36, 965.
38. Kim, H.-S.; Kim, S.; Kim, H.-J.; Yang, H.-S. *Thermochim Acta* 2006, 451, 181.
39. Yao, F.; Wu, Q.; Lei, Y.; Guo, W.; Xu, Y. *Polym Degrad Stab* 2008, 93, 90.
40. Di Blasi, C. *Prog. Energy Combust Sci* 2008, 34, 47.



Contents lists available at SciVerse ScienceDirect

Bioresource Technology

journal homepage: [www.elsevier.com/locate/biortech](http://www.elsevier.com/locate/biortech)

## Thermal decomposition of wood: Influence of wood components and cellulose crystallite size

Matheus Poletto<sup>a,b,\*</sup>, Ademir J. Zattera<sup>b</sup>, Maria M.C. Forte<sup>a</sup>, Ruth M.C. Santana<sup>a</sup>

<sup>a</sup> Programa de Pós-graduação em Engenharia de Minas, Metalúrgica e de Materiais, Universidade Federal do Rio Grande do Sul, Av. Bento Gonçalves 9500, 91501-970 Porto Alegre, RS, Brazil

<sup>b</sup> Laboratório de Polímeros, Universidade de Caxias do Sul, Rua Francisco Getúlio Vargas 1130, 95070-560 Caxias do Sul, RS, Brazil

### ARTICLE INFO

#### Article history:

Received 10 October 2011

Received in revised form 25 November 2011

Accepted 28 November 2011

Available online 21 January 2012

#### Keywords:

Wood

Cellulose

Crystallite size

Thermal analysis

X-ray diffractometry

### ABSTRACT

The influence of wood components and cellulose crystallinity on the thermal degradation behavior of different wood species has been investigated using thermogravimetry, chemical analysis and X-ray diffraction. Four wood samples, *Pinus elliottii* (PIE), *Eucalyptus grandis* (EUG), *Mezilaurus itauba* (ITA) and *Dipteryx odorata* (DIP) were used in this study. The results showed that higher extractives contents associated with lower crystallinity and lower cellulose crystallite size can accelerate the degradation process and reduce the wood thermal stability. On the other hand, the thermal decomposition of wood shifted to higher temperatures with increasing wood cellulose crystallinity and crystallite size. These results indicated that the cellulose crystallite size affects the thermal degradation temperature of wood species.

© 2012 Published by Elsevier Ltd.

### 1. Introduction

Biomass has been recognized as a potential renewable energy and a substitute for the declining supply of fossil fuel resources (Kim et al., 2010a; Wongsiriamnuay and Tippayawong, 2010; Shen and Gu, 2009). Common sources of biomass include several kinds of wood, agricultural crops and natural fibers (Wongsiriamnuay and Tippayawong, 2010). The interest in biomass as an alternative energy is increasing as a result of its continuous regeneration. On the other hand, biomass in a fiber or particulate form has been used as a reinforcing filler in thermoplastic composite materials (Poletto et al., 2011a; Ashori and Nourbakhsh, 2010; Liu et al., 2009). These lignocellulosic materials are in general suitable for addition to reinforced plastics due to their relative high strength and stiffness, low cost, low density, low CO<sub>2</sub> emission and biodegradability besides being annually renewable (Nachtigall et al., 2007; Araújo et al., 2008). However, they present limitations such as moisture adsorption and low thermal stability (Araújo et al., 2008; Poletto et al., 2010).

Wood is a polymeric composite, which essentially contains cellulose, hemicellulose, lignin and extractives. Wood degradation

takes place at a relatively low temperature, around 200 °C (Araújo et al., 2008; Poletto et al., 2010). As a result, wood is subjected to thermal degradation during composite processing with the majority of the thermoplastic polymers (Liu et al., 2009). The degradation of wood resulting from high processing temperatures may lead to undesirable properties, such as odor and browning, along with a reduction in mechanical properties of the developed composite (Liu et al., 2009; Shebani et al., 2009). Therefore, it is of practical significance to understand and predict the thermal decomposition process of wood so that this knowledge can aid to better design a composite-obtaining process and estimate the influence of the thermal decomposition of wood on composite properties (Yao et al., 2008).

Due to the complexity of the thermal decomposition reactions of wood, extensive researches have determined individual behaviors of the main wood components. Órfão et al. (1999) and Órfão and Figueiredo (2001) introduced three independent reaction models to describe the pyrolysis kinetics of some lignocellulosic materials, while Branca et al. (2005) and Di Blasi (2008) used three parallel reactions to describe the fast pyrolysis process of wood. Grønli et al. (2002) showed a devolatilization mechanism of hardwoods and softwoods consisting of three parallel reactions resulting from the degradation of the three main components of wood.

A considerable amount of work has been reported on the study of wood decomposition as mentioned above. However, the literature lacks works on the influence of wood components and wood cellulose crystallinity on the degradation of wood species. In this

\* Corresponding author at: Programa de Pós-graduação em Engenharia de Minas, Metalúrgica e de Materiais, Universidade Federal do Rio Grande do Sul, Av. Bento Gonçalves 9500, 91501-970 Porto Alegre, RS, Brazil. Tel.: +55 54 3218 2108; fax: +55 54 3218 2253.

E-mail address: [mpoletto1@ucs.br](mailto:mpoletto1@ucs.br) (M. Poletto).



context, this work has evaluated how the wood components and wood cellulose crystallinity influence wood thermal stability. Four different wood species from Brazil were investigated using chemical analysis, X-ray diffraction and thermogravimetric analysis.

## 2. Methods

### 2.1. Materials

The wood flour samples used in this study were obtained from wastes of the Brazil lumber industry. The species investigated were *Pinus elliottii*, *Eucalyptus grandis*, *Mezilaurus itauba* and *Dipteryx odorata*. Samples having particle size between 200 and 300  $\mu\text{m}$  were dried in a vacuum oven at 105 °C for 24 h before the thermogravimetric analysis.

### 2.2. Chemical analysis

Benzene and absolute ethanol purchased from Vetec Chemical were used to determine the amount of organic extractives in the wood samples. Sulphuric acid purchased from Vetec Chemical was used for insoluble lignin determination. The wood extractives were eliminated from wood via Soxhlet extraction in triplicate using: ethanol/benzene and ethanol and hot water according to the Tappi T204 cm-97 standard. The Klason lignin content was determined according to the Tappi T222 om-02 standard. The determination of the ash content was carried out at 600 °C for 1 h in a muffle furnace, based on Tappi T211 om-02. The holocellulose content (cellulose + hemicellulose) was determined by difference.

### 2.3. X-ray diffraction (XRD)

X-ray diffractograms were collected using a sample holder mounted on a Shimadzu diffractometer (XRD-6000), with monochromatic Cu K $\alpha$  radiation ( $\lambda = 0.1542 \text{ nm}$ ), the generator operating at 40 kV and 30 mA. Intensities were measured in the range of  $5 < 2\theta < 35^\circ$ , typically with scan steps of  $0.05^\circ$  and 2 s/step ( $1.5^\circ \text{ min}^{-1}$ ). Peak separations were carried out using Gaussian deconvolution. After deconvolution it is possible to calculate and compare several parameters. The  $d$ -spacings were calculated using the Bragg equation [17,18].

The crystalline index (Eq. (1)), proposed by Hermans et al. (Wada and Okano, 2001; Popescu et al., 2011) is:

$$\text{Cr} \cdot \text{I} = \frac{A_{\text{cryst}}}{A_{\text{total}}} \quad (1)$$

where Cr.I. is the crystalline index,  $A_{\text{cryst}}$  is the sum of crystalline band areas, and  $A_{\text{total}}$  is the total area under the diffractograms.

The second approach used to determine the crystalline index (Eq. (2)) was the empirical method proposed by Segal et al. (1959) (Wada and Okano, 2001; Gümüşkaya et al., 2003):

$$\text{C} \cdot \text{I} = \frac{I_{002} - I_{\text{am}}}{I_{002}} \times 100 \quad (2)$$

The apparent crystallite size ( $L$ ) (Eq. (3)) was calculated using the Scherrer equation (Popescu et al., 2011):

$$L = \frac{K \cdot \lambda}{\beta \cdot \cos \theta} \quad (3)$$

where  $K$  is a constant of value 0.94,  $\lambda$  is the X-ray wavelength (0.1542 nm),  $\beta$  is the half-height width of the diffraction band and  $\theta$  is the Bragg angle corresponding to the (200) plane.

The surface chains occupy a layer approximately 0.57 nm thick so the proportion of crystallite interior chains (Popescu et al., 2011; Davidson et al., 2004) is:

$$X = \frac{(L - 2h)^2}{L^2} \quad (4)$$

where  $L$  is the apparent crystallite size for the reflection of plane (200), and  $h = 0.57 \text{ nm}$  is the layer thickness of the surface chain.

### 2.4. Thermogravimetric analysis (TGA)

The thermogravimetric analysis (TGA50 – Shimadzu) was carried out under  $\text{N}_2$  atmosphere with a purge gas flow of  $50 \text{ cm}^3 \text{ min}^{-1}$  from 25 to 800 °C. Approximately 10 mg of each sample was used. The heating rate of the analysis was  $10^\circ \text{C min}^{-1}$ .

## 3. Results and discussions

### 3.1. Chemical composition of wood species

In order to determine the effect of the chemical composition of wood species under study on the wood thermal stability the amount of holocellulose, lignin and extractives was determined for all samples. The initial wood degradation temperature is expected to be related to the heat stability of the individual wood components and differences in thermal stability among wood species can be attributed to the variation in chemical composition (Poletto et al., 2010; Shebani et al., 2008). On the other hand, the fundamental differences among wood species are found in the types, size, proportions, pits and arrangements of the different cells that compose wood (Popescu et al., 2011). These differences might affect the crystallinity and crystallite size of the wood species with impacts on wood thermal stability.

The results for the chemical composition of the wood species studied are presented in Table 1. The holocellulose and lignin contents were higher for the EUG and PIE species than for the DIP and ITA species. The PIE had the highest lignin content around 34% while ITA had the lowest, 28%. The holocellulose content of wood is generally around 60–70%, while the lignin is usually in the range of 20–35% (Rowell, 2005; Klyosov, 2007). However, ITA and DIP contain three times more extractives than EUG and PIE. In general, the extractives content varies between 2% and 5% but it can exceed 15% in some wood species (Shebani et al., 2008; Klyosov, 2007). The ash content of the DIP species was higher than that of the other species studied and this value is probably associated with higher amounts of mineral salts in this wood species than in the other species evaluated. The inorganic content of a wood species is usually referred to as its ash content, which is an approximate measure of its mineral salts and other inorganic matters content. It normally varies between 0.2% and 0.5% in wood (Rowell, 2005; Klyosov, 2007), but tropical species often exceed this range (Branca and Di Blasi, 2003; Hon and Shiraiishi, 2001).

**Table 1**  
Chemical composition of the investigated wood species.

Wood species	Holocellulose (%)	Lignin (%)	Extractives (%)	Ash (%)
<i>Eucalyptus grandis</i> (EUG)	62.7 $\pm$ 1.4	32.1 $\pm$ 1.0	4.1 $\pm$ 0.2	1.1 $\pm$ 0.3
<i>Pinus elliottii</i> (PIE)	61.2 $\pm$ 1.1	33.8 $\pm$ 1.0	4.5 $\pm$ 0.1	0.8 $\pm$ 0.1
<i>Dipteryx odorata</i> (DIP)	57.1 $\pm$ 0.6	30.4 $\pm$ 0.4	11.1 $\pm$ 0.1	1.5 $\pm$ 0.2
<i>Mezilaurus itauba</i> (ITA)	57.8 $\pm$ 1.0	28.0 $\pm$ 0.3	13.6 $\pm$ 0.7	0.7 $\pm$ 0.1

3.2. X-ray diffraction

The X-ray diffraction is a method used generally to evaluate the degree of crystallinity in several materials. Among wood components, only cellulose is crystalline, while hemicellulose and lignin are non-crystalline (John and Thomas, 2008). The free hydroxyl groups present in the cellulose macromolecules are likely to be involved in a number of intramolecular and intermolecular hydrogen bonds, which may give rise to various ordered crystalline arrangements (Popescu et al., 2011; Poletto et al., 2011b).

Fig. 1 shows the X-ray diffractograms of the wood samples studied. In order to examine the intensities of the diffraction bands, establish the crystalline and amorphous areas more exactly and determine the crystallite sizes the diffractograms were deconvoluted using Gaussian profiles. The peak intensities and peak broadening differ from one species to another. The more pronounced difference occurs at the peak range between 21.90° and 22.20° 2θ reflection assigned with a crystallographic plane of cellulose. The peak area at 21.90–22.20° 2θ reflection follow the sequence DIP > ITA > EUG > PIE, as can be seen in Fig. 1.

Crystallographic planes are labeled according to the native cellulose structure as described by Wada et al. (2001). After deconvolution, all diffractograms show the 14.8–15.3° 2θ reflection assigned to the (110) crystallographic plane, the 16.20–16.30° 2θ reflection assigned to the (110) crystallographic plane, the 18.30–18.40° 2θ reflection assigned to the amorphous phase and the 21.90–22.20° 2θ reflection assigned to the (200) crystallographic plane of cellulose I (Popescu et al., 2011; Wada et al., 2001). Fig. 2 shows a model to represent the cellulose chains and the crystallographic planes described above.

Wood cellulose is known to be a composite of two distinct crystalline structures, namely I<sub>α</sub> and I<sub>β</sub>. The I<sub>α</sub> and I<sub>β</sub> structures are assigned to triclinic and monoclinic unit cells, respectively (Poletto et al., 2011b; Wada et al., 2001). The d-spacings of wood celluloses calculated from X-ray diffractometry profiles were 0.579–0.599 nm for d<sub>(110)</sub> and 0.542–0.554 nm for d<sub>(110)</sub>, as can be seen in Table 2. These figures indicated that wood cellulose samples used in this study are all I<sub>β</sub>-type cellulose (Wada and Okano, 2001; Wada et al., 2001). These values are significantly different from the d-spacings of the I<sub>α</sub>-rich type celluloses, 0.610–0.617 nm for d<sub>(110)</sub> and 0.530–0.541 nm for d<sub>(110)</sub> (Kim et al., 2010a,b). These data support previous results from diffraction methods stating that the monoclinic structure (I<sub>β</sub>) is dominant in wood cellulose (Wada et al., 2001; Kim et al., 2010a,b).

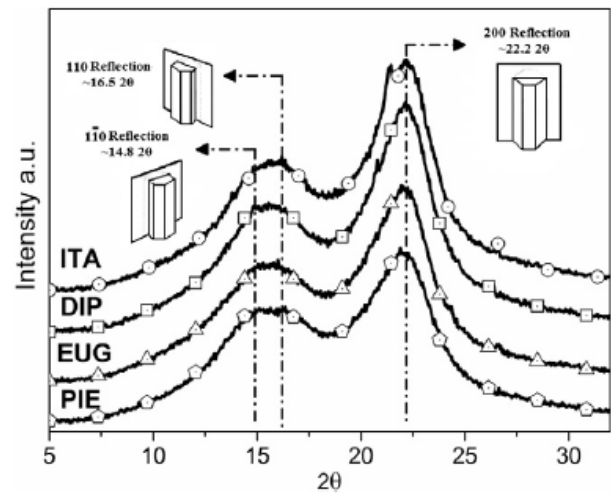


Fig. 1. X-ray diffractograms of wood species studied with corresponding crystal planes, adapted from (Howell, 2008), and most common 2θ values.

The degree of cellulose crystallinity is one of the most important crystalline structure parameters. The rigidity of cellulose fibers increases and their flexibility decreases with increasing ratio of crystalline to amorphous regions (Gümüşkaya et al., 2003). The crystallinity index calculated according to the Hermans (Eq. (1)) and Segal methods (Eq. (2)) showed that the crystallinity of the DIP and ITA species was higher than that of EUG and PIE, as presented in Table 3. These differences are confirmed when the values of the crystallite size along the three crystallographic planes are taken into consideration. Crystallinity indices increased with increasing crystallite sizes because the crystallites surface corresponding to amorphous cellulose regions diminished (Kim et al., 2010a,b). These results indicated that DIP and ITA contain a more ordered cellulose structure than EUG and PIE.

The values of X were used as estimates of the fraction of cellulose chains contained in the interior of the crystallites (Newman, 1999). Once again, DIP and ITA species showed higher values than EUG and PIE. This result confirms that DIP and ITA wood species contain much more cellulose chains in a highly organized form in the interior of the cellulose crystallite. This can lead to higher hydrogen bond intensity among neighboring cellulose chains

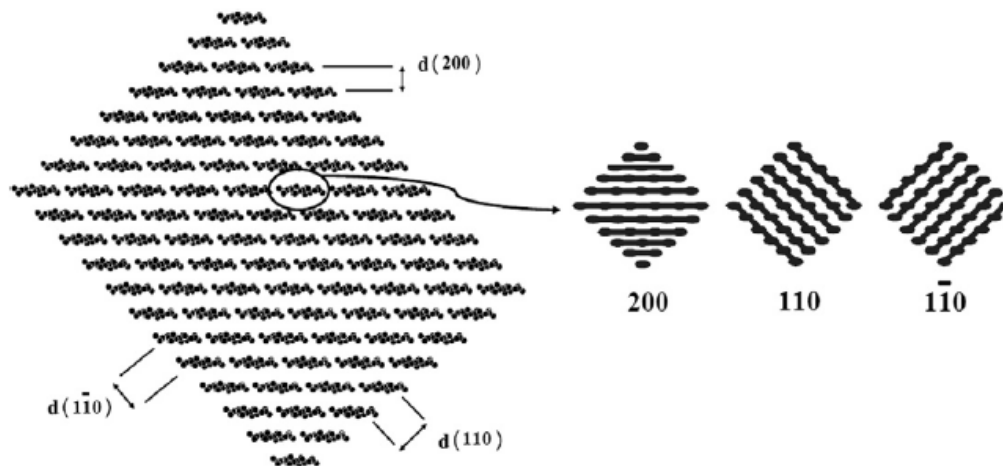


Fig. 2. Model used to represent cellulose chains (left), showing the d-spacings along the cellulose structure, adapted from (Newman, 2008). Lines indicated the crystallographic planes in native cellulose (right), each ellipse represents a chain normal to the paper, adapted from (Newman, 1999).



**Table 2**Band position ( $2\theta$ ) and d-spacings of crystalline and amorphous cellulose regions for the wood samples studied.

Wood species	(110)		(110)		Amorphous	(200)	
	$2\theta$	$d$ (nm)	$2\theta$	$d$ (nm)		$2\theta$	$d$ (nm)
<i>Eucalyptus grandis</i> (EUG)	15.30	0.579	16.01	0.554	18.30	21.95	0.405
<i>Pinus elliottii</i> (PIE)	15.10	0.587	16.35	0.542	18.40	21.90	0.406
<i>Dipteryx odorata</i> (DIP)	14.91	0.595	16.30	0.544	18.40	22.15	0.402
<i>Mezilaurus itauba</i> (ITA)	14.80	0.599	16.20	0.547	18.35	22.20	0.401

**Table 3**

Parameters obtained from the XRD analysis of the wood samples studied.

Wood species	$L(1\bar{1}0)$ (nm)	$L(110)$ (nm)	$L(200)$ (nm)	Cr.I.	C.I.	$X$
<i>Eucalyptus grandis</i> (EUG)	1.72	2.29	2.11	34.4	49.3	0.21
<i>Pinus elliottii</i> (PIE)	1.71	2.44	1.92	34.1	43.4	0.17
<i>Dipteryx odorata</i> (DIP)	1.97	2.30	2.18	43.0	55.7	0.23
<i>Mezilaurus itauba</i> (ITA)	1.81	2.13	2.23	37.8	52.7	0.24

result in a more packed cellulose structure besides higher crystallinity. On the other hand, the thermal stability of cellulose was found to depend mainly on its crystallinity index, crystallite size and degree of polymerization (Poletto et al., 2011b; Kim et al., 2010b; Nada et al., 2000).

### 3.3. Thermogravimetric analysis

Fig. 3 shows the results of the thermogravimetric analysis performed on the different wood species. Fig. 3(a) gives the percentage of weight loss as a function of temperature, while Fig. 3(b) presents the derivative thermogravimetric curves. Water loss is observed around 100 °C, and further thermal degradation takes place as a two-step process. In the first step, the degradation of hemicellulose takes place at around 300 °C and a slight shoulder in the DTG curve can be seen in Fig. 3(b) for all wood species studied. At around 350 °C the main degradation of cellulose occurs and a prominent peak appears at the temperature corresponding to the maximum decomposition rate. According to Kim et al. (2006) the depolymerization of hemicellulose occurs between 180 and 350 °C, the random cleavage of the glycosidic linkage of cellulose between 275 and 350 °C and the degradation of lignin between 250 and 500 °C. The higher activity of hemicellulose in thermal decomposition might be attributed to its chemical structure (John and Thomas, 2008; Yang et al., 2006). Hemicellulose has a random amorphous structure and it is easily hydrolyzed (John and Thomas, 2008; Yang et al., 2006). In contrast, the cellulose molecule is a very long polymer of glucose units, and its crystalline regions improve the thermal stability of wood (Yang et al., 2006). Lignin is different from hemicellulose and cellulose because it is composed of three kinds of benzene-propane units, being heavily cross-linked and having very high molecular weight (John and Thomas, 2008; Yang et al., 2006). The thermal stability of lignin is thus very high, and it is difficult to decompose (Yang et al., 2006).

As can be seen in detail in Fig. 3(a) at temperatures around 180–190 °C the ITA wood shows a more significant weight loss. This behavior might be associated with the highest content of extractives in this wood, around 14% as presented in Table 1. Extractives are compounds of lower molecular mass as compared to cellulose, and can promote ignitability of the wood at lower temperatures as a result of their higher volatility and thus accelerate the degradation process. In this way, the degradation of one component may accelerate the degradation of the other wood components. Grønli et al. (2002) and Shebani et al. (2008) observed that wood degradation at low temperatures is usually associated with extractive decomposition. On the other hand, the individual chemical components of wood behave differently if they are isolated or intimately combined

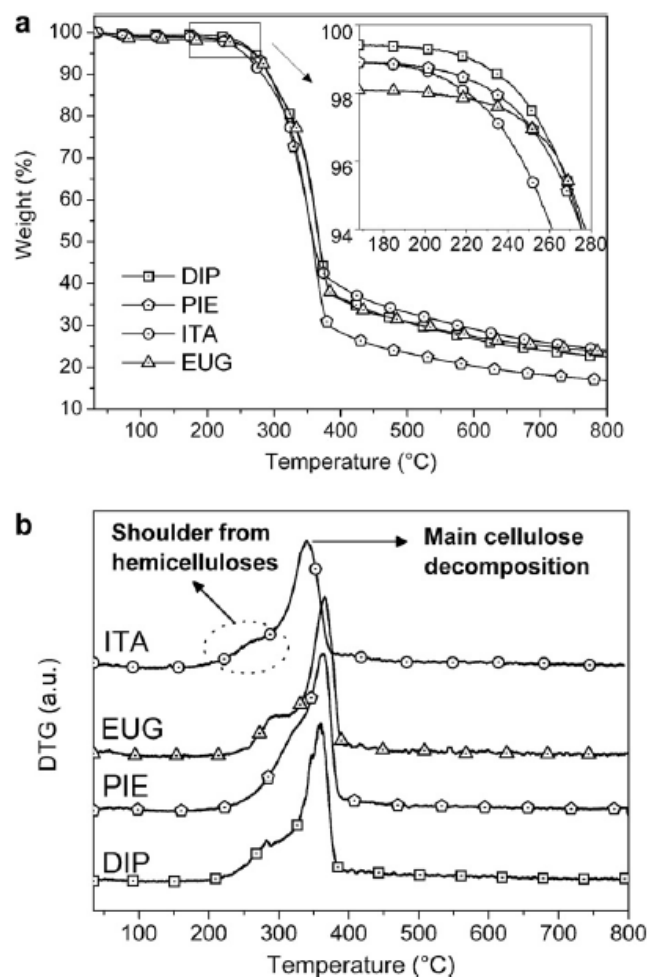


Fig. 3. TGA (a) and DTG (b) curves for the different wood species studied.

within each single cell of the wood structure (Popescu et al., 2010). However, the DIP wood that contains around 11% of extractives showed higher thermal stability than ITA. This behavior may be related to the higher content of lignin in DIP relative to that of ITA and the higher crystallinity index and crystallite size in this wood, as can be seen in Table 3.



**Table 4**

Thermal degradation temperatures, T shoulder, DTG peak and % residue at 800 °C for the wood species under study.

Wood species	T <sub>i</sub> (°C) 3 wt.% loss	T shoulder (°C)	DTG peak (°C)	Residue at 800 °C (%)
<i>Eucalyptus grandis</i> (EUG)	250	291	364	23.6
<i>Pinus elliottii</i> (PIE)	251	322	367	16.8
<i>Dipteryx odorata</i> (DIP)	257	289	368	22.4
<i>Mezilaurus itauba</i> (ITA)	237	275	350	24.1

The initial weight loss temperature,  $T_i$ , of all samples, is considered as the temperature at which the sample loses 3% of its weight, as showed in Table 4. The lowest  $T_i$  value was attributed to ITA, as can be seen in detail in Fig. 3(a). This might be associated with higher volatility of extractives and hemicellulose in this wood. The highest  $T_i$  values were observed for the EUG, PIE and DIP wood species. On the other hand, EUG, ITA and DIP had a significant amount of residue at 800 °C probably due to higher inorganic contents in these three wood species.

Wood is commonly used as filler only in polymers that are processed at temperatures at around 200 °C (Araújo et al., 2008; Shebani et al., 2009). Accounting to this fact, the detail in Fig. 3(a) showed that ITA and PIE woods initiate a more pronounced degradation process at around 180–190 °C and 190–200 °C, respectively. The low degradation temperature of ITA and PIE samples can lead to undesirable composite properties, such as browning and decreasing of the mechanical strength when processed at temperatures above 200 °C. On the other hand, DIP and EUG woods initiate a more pronounced degradation process at around 220 °C which can lead to thermoplastic polymer composites with higher mechanical and thermal properties by increasing the processing temperature range.

Because the temperature intervals of hemicellulose, cellulose and lignin decomposition partially overlap each other, the hemicellulose and/or amorphous cellulose decomposition step usually appears as a more or less pronounced shoulder instead of a well-defined peak. This shoulder is better evidenced for the ITA, EUG and DIP wood species, as can be seen in Fig. 3(b). For PIE the shoulder occurs at a higher temperature than for the other wood species. This result may be a consequence, on the one hand, of lower extractives volatility and on the other hand, of lower hemicellulose reactivity. The main degradation of cellulose occurs at higher temperatures for EUG, PIE and DIP respectively. For EUG the main degradation temperature of cellulose occurs at 364 °C and might be related to the higher content of holocellulose and lower content of extractives in this wood, see Table 1. The contents of holocellulose and extractives in PIE wood were comparable to those of EUG, however the cellulose main degradation temperature for this wood occurs at 367 °C. One explanation for this fact is the higher PIE cellulose crystallite size at the (110) crystallographic plane, which may improve thermal stability. The DIP extractives amount is higher while the content of holocellulose is lower than those of EUG and PIE. However, it is interesting to note that the thermal stability was more pronounced and the main decomposition of cellulose was higher for DIP as compared to EUG and PIE. This behavior may be associated with the highest crystalline index and higher crystallite size of cellulose in this wood. In a recent study, Kim et al. (2010b) showed that the thermal decomposition of cellulose shifted to higher temperatures with increasing crystallinity index and crystallite size.

Some models of the cellulose thermal decomposition in wood have been suggested. Kim et al. (2010b) discussed three possible models for thermal decomposition of wood cellulose crystallites: (a) where decomposition preferentially proceeds along the fiber axis; (b) where a crystallite that once starts to decompose undergoes rapid decomposition while the other crystallites remain largely

intact, and (c) a combination of the (a) and (b) models. Zickler et al. (2007) studied the thermal decomposition of cellulose in wood at various temperatures by in situ X-ray diffraction using synchrotron radiation. The authors proposed that the thermal decomposition of cellulose in wood occurs mainly via a thermally activated decrease of the fibril cellulose diameter. This decomposition is followed by a random breaking of the cellulose fibrils into shorter length pieces as a consequence of the extremely anisotropic nature of the higher hydrogen bonding forces in cellulose crystallites (Zickler et al., 2007). As a result, a higher amount of hydrogen bond between neighboring cellulose chains may be resulted from a more packed cellulose structure which can lead out to higher crystallinity and thermal stability, as observed in the case of DIP sample. In addition, intramolecular hydrogen bonds stabilize the cellulose molecules and may inhibit thermal expansion along this direction (Hidaka et al., 2010) improving the wood thermal stability.

Although the decomposition of wood is a complex process and involves a series of competitive and/or consecutive reactions. It might be difficult to distinguish and model the thermal decomposition behavior of each specific component in wood due to the complexity of growth of wood which causes variance in components content, crystal structure and chemical composition from one species to another (Poletto et al., 2010; Yao et al., 2008; Di Blasi, 2008).

#### 4. Conclusions

Chemical analysis reveals that DIP and ITA contain higher amount of extractives than EUG and PIE. The X-ray diffractometry results showed that DIP and ITA contain much more cellulose chains in highly organized form in the interior of the crystallite, which can lead to higher crystallinity. The combined results showed that higher extractives contents associated with lower crystallinity and lower crystallite size accelerate the degradation process and reduce wood thermal stability. However, thermal decomposition of DIP shifted to higher temperatures with increasing cellulose crystallinity and crystallite size. These results indicated that cellulose crystallite size affects the wood thermal degradation temperature.

#### Acknowledgement

The authors are grateful to Prof. Ricardo Campomanes from Universidade Federal de Mato Grosso (UFMT) for supplying the wood samples and CAPES for financial support.

#### References

- Araújo, J.R., Waldman, W.R., De Paoli, M.A., 2008. Thermal properties of high density polyethylene composites with natural fibres: coupling agent effect. *Polym. Degrad. Stab.* 93, 1770–1775.
- Ashori, A., Nourbakhsh, A., 2010. Reinforced polypropylene composites: effects of chemical compositions and particle size. *Bioresour. Technol.* 101, 2515–2519.
- Branca, C., Albano, A., Di Blasi, C., 2005. Critical evaluation of global mechanisms of wood devolatilization. *Thermochim. Acta* 429, 133–141.
- Branca, C., Di Blasi, C., 2003. Global kinetics of Wood char devolatilization and combustion. *Energy Fuels* 17, 1609–1615.

- Davidson, T.C., Newman, R.H., Ryan, M.J., 2004. Variations in the fibre repeat between samples of cellulose I from different sources. *Carbohydr. Res.* 339, 2889–2893.
- Di Blasi, C., 2008. Modeling chemical and physical process of wood and biomass pyrolysis. *Prog. Energy Combust. Sci.* 34, 47–90.
- Grønli, M.G., Várhegyi, G., Di Blasi, C., 2002. Thermogravimetric analysis and devolatilization kinetics of wood. *Ind. Eng. Chem. Res.* 41, 4201–4208.
- Gümüşkaya, E., Usta, M., Kirei, H., 2003. The effects of various pulping conditions on crystalline structure of cellulose in cotton linters. *Polym. Degrad. Stab.* 81, 559–564.
- Hidaka, H., Kim, U.-J., Wada, M., 2010. Synchrotron X-ray fiber diffraction study on the thermal expansion behavior of cellulose crystals in tension wood of Japanese poplar in the low-temperature region. *Holzforschung* 64, 167–171.
- Hon, D.N.-S., Shiraishi, N., 2001. *Wood and Cellulosic Chemistry*. Marcel Dekker, Inc., New York.
- Howell, C.L., 2008. Understanding wood biodegradation through the characterization of crystalline cellulose nanostructures. Doctoral thesis. University of Maine.
- John, M.J. & Thomas, S., 2008. Biofibres and biocomposites. *Carbohydr. Polym.* 71, 343–364.
- Kim, S.-S., Kim, J., Park, Y.-H., Park, Y.-K., 2010a. Pyrolysis kinetics and decomposition characteristics of pine trees. *Bioresour. Technol.* 101, 9797–9802.
- Kim, U.-J., Eom, S.H., Wada, M., 2010b. Thermal decomposition of native cellulose: influence on crystallite size. *Polym. Degrad. Stab.* 95, 778–781.
- Kim, H.-S., Kim, S., Kim, H.-J., Yang, H.-S., 2006. Thermal properties of bio-flour-filled polyolefin composites with different compatibilizing agent type and content. *Thermochim. Acta* 451, 181–188.
- Klyosov, A.A., 2007. *Wood-Plastic Composites*. John Wiley & Sons, Inc., New Jersey.
- Liu, H., Wu, Q., Zhang, Q., 2009. Preparation and properties of banana fiber-reinforced composites based on high density polyethylene (HDPE)/Nylon-6 blends. *Bioresour. Technol.* 100, 6088–6097.
- Nachtigall, S.M.B., Cerveira, G.S., Rosa, S.M.L., 2007. New polymeric-coupling agent for polypropylene/wood-flour composites. *Polym. Test.* 26, 619–628.
- Nada, A.-A.M.A., Kamel, S., El-Sakhawy, M., 2000. Thermal behavior and infrared spectroscopy of cellulose carbamates. *Polym. Degrad. Stab.* 70, 347–355.
- Newman, R.H., 2008. Simulation of X-ray diffractograms relevant to the purported polymorphs cellulose IV<sub>1</sub> and IV<sub>2</sub>. *Cellulose* 15, 769–778.
- Newman, R.H., 1999. Estimation of the lateral dimensions of cellulose crystallites using <sup>13</sup>C NMR signal strengths. *Solid State Nucl. Magn. Reson.* 15, 21–29.
- Órfão, J.J.M., Antunes, F.J.A., Figueiredo, J.L., 1999. Pyrolysis kinetics of lignocellulosic materials – three independent reactions model. *Fuel* 78, 349–358.
- Órfão, J.J.M., Figueiredo, J.L., 2001. A simplified method for determination of lignocellulosic materials pyrolysis kinetics from isothermal thermogravimetric experiments. *Thermochim. Acta* 380, 67–78.
- Poletto, M., Dettenborn, J., Zeni, M., Zattera, A.J., 2011a. Characterization of composites based on expanded polystyrene wastes and wood flour. *Waste Manage.* 31, 779–784.
- Poletto, M., Pistor, V., Zeni, M., Zattera, A.J., 2011b. Crystalline properties and decomposition kinetics of cellulose fibers in wood pulp obtained by two pulping process. *Polym. Degrad. Stab.* 96, 679–685.
- Poletto, M., Dettenborn, J., Pistor, V., Zeni, M., Zattera, A.J., 2010. Materials produced from plant biomass. Part I: evaluation of thermal stability and pyrolysis of wood. *Mat. Res.* 13, 375–379.
- Popescu, C.-M., Popescu, M.-C., Vasile, C., 2010. Structural changes in biodegradable lime wood. *Carbohydr. Polym.* 79, 362–372.
- Popescu, M.-C., Popescu, C.-M., Lisa, G., Sakata, Y., 2011. Evaluation of morphological and chemical aspects of different wood species by spectroscopy and thermal methods. *J. Mol. Struct.* 988, 65–72.
- Rowell, R., 2005. *Handbook of Wood Chemistry and Wood Composites*. CRC Press, Boca Raton.
- Segal, L., Creely, L., Martin, A.E., Conrad, C.M., 1959. An empirical method for estimating the degree of crystallinity of native cellulose using X-ray diffractometer. *Text. Res. J.* 29, 786–794.
- Shebani, A.N., van Reenen, A.J., Meincken, M., 2009. The effect of wood extractives on the thermal stability of different wood-LLDPE composites. *Thermochim. Acta* 481, 52–56.
- Shebani, A.N., van Reenen, A.J., Meincken, M., 2008. The effect of wood extractives on the thermal stability of different wood species. *Thermochim. Acta* 471, 43–50.
- Shen, D.K., Gu, S., 2009. The mechanism for thermal decomposition of cellulose and its main products. *Bioresour. Technol.* 100, 6496–6504.
- Wada, M., Okano, T., 2001. Localization of I<sub>α</sub> and I<sub>β</sub> phases in algal cellulose revealed by acid treatments. *Cellulose* 8, 183–188.
- Wada, M., Okano, T., Sugiyama, J., 2001. Allomorphs of native crystalline cellulose I evaluated by two equatorial d-spacings. *J. Wood Sci.* 47, 124–128.
- Wongsiriamnuay, T., Tippayawong, N., 2010. Non-isothermal pyrolysis characteristics of giant sensitive plants using thermogravimetric analysis. *Bioresour. Technol.* 101, 5638–5644.
- Yao, F., Wu, Q., Lei, Y., Guo, W., Xu, Y., 2008. Thermal decomposition kinetics of natural fibers: Activation energy with dynamic thermogravimetric analysis. *Polym. Degrad. Stab.* 93, 90–98.
- Yang, H., Yan, R., Chen, H., Zheng, C., Lee, D.H., Liang, D.T., 2006. In-depth investigation of biomass pyrolysis based on three major components: hemicellulose, cellulose and lignin. *Energy Fuels* 20, 388–393.
- Zickler, G.A., Wagermaier, W., Funari, S.S., Burghammer, M., Paris, O., 2007. *In situ* X-ray diffraction investigation of thermal decomposition of wood cellulose. *J. Anal. Appl. Pyrolysis* 80, 134–140.





Contents lists available at SciVerse ScienceDirect

Bioresource Technology

journal homepage: [www.elsevier.com/locate/biortech](http://www.elsevier.com/locate/biortech)

## Thermal decomposition of wood: Kinetics and degradation mechanisms

Matheus Poletto<sup>a,b,\*</sup>, Ademir J. Zattera<sup>b</sup>, Ruth M.C. Santana<sup>a</sup>

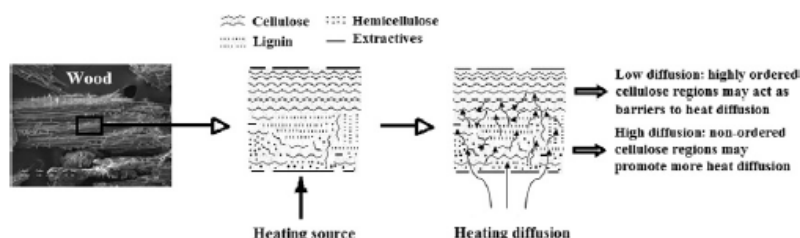
<sup>a</sup> Programa de Pós-graduação em Engenharia de Minas, Metalúrgica e de Materiais/Universidade Federal do Rio Grande do Sul, Av. Bento Gonçalves 9500, 91501-970 Porto Alegre/RS, Brazil

<sup>b</sup> Laboratório de Polímeros/Universidade de Caxias do Sul, Rua Francisco Getúlio Vargas 1130, 95070-560 Caxias do Sul/RS, Brazil

### HIGHLIGHTS

- ▶ Higher extractives content accelerate the wood degradation process.
- ▶ Higher organized cellulose regions prevent wood thermal degradation.
- ▶ Wood degradation mechanism is mainly governed by diffusion process.

### GRAPHICAL ABSTRACT



### ARTICLE INFO

#### Article history:

Received 29 June 2012

Received in revised form 27 August 2012

Accepted 28 August 2012

Available online 13 September 2012

#### Keywords:

Wood  
Cellulose  
Crystallinity  
Thermal analysis  
Kinetic analysis

### ABSTRACT

The influence of wood components and cellulose crystallinity on the kinetic degradation of different wood species has been investigated using thermogravimetry. Four wood species were studied: *Pinus elliottii* (PIE), *Eucalyptus grandis* (EUG), *Mezilaurus itauba* (ITA) and *Dipteryx odorata* (DIP). Thermogravimetric results showed that higher extractive contents in the wood accelerate the degradation process and promote an increase in the conversion values at low temperatures. Alternatively, the results indicated that the cellulose crystallinity inhibits wood degradation; organized cellulose regions slow the degradation process because the well-packed cellulose chains impede heat diffusion, which improves the wood's thermal stability. The wood degradation mechanism occurs by diffusion processes when the conversion values are below 0.4. When the conversion values are above 0.5, the degradation is a result of random nucleation with one nucleus in each particle.

© 2012 Elsevier Ltd. All rights reserved.

### 1. Introduction

Sustainable heat and power generation from biomass are at the center of scientific and industrial interests, owing to the increasing awareness of the diminution of fossil fuels and the higher sensibility toward environmental preservation from pollutants generated by energetic systems (Di Blasi, 2008). Biomass is a source of short-cycle carbon, which is of utmost importance for future energy needs (Wongsiriamnuay and Tippayawong, 2010a). Wood is the main source of biomass (Di Blasi, 2008). Thus, wood remains one of the most important biomass materials for several applica-

tions because of its renewability, high-yield applications and appropriate characteristics (Wongsiriamnuay and Tippayawong, 2010a). Additionally, the growth of wood reduces the CO<sub>2</sub> in the atmosphere through photosynthesis (Wongsiriamnuay and Tippayawong, 2010a; Shuping et al., 2010).

From the chemical point of view, wood is a composite material comprised of cellulose, hemicellulose and lignin, along with smaller quantities of extractives and inorganic matter. From the physical point of view, wood is a complex structure with anisotropic properties (Di Blasi, 2008; Popescu et al., 2011). The chemical and physical properties of wood such as moisture content, chemical composition, density and crystallinity are factors that affect the characteristics of thermal decomposition and degradation kinetics (Di Blasi, 2008; Órfão et al., 1999; Popescu et al., 2011).

Pyrolysis can be described as the biomass conversion by heat in absence of oxygen in a relatively low range of temperatures (300–600 °C) which results in the production fuel gasses, charcoal and

\* Corresponding author at: Programa de Pós-graduação em Engenharia de Minas, Metalúrgica e de Materiais/Universidade Federal do Rio Grande do Sul, Av. Bento Gonçalves 9500, 91501-970 Porto Alegre/RS, Brazil. Tel.: +55 54 321 82108; fax: +55 54 321 82253.

E-mail address: [mpolett1@ucs.br](mailto:mpolett1@ucs.br) (M. Poletto).

bio-oil (Sanchez-Silva et al., 2012; Órfão et al., 1999). Also, pyrolysis is of special interest since it is a prior step in combustion and gasification processes (Sanchez-Silva et al., 2012). So, it seems essential to obtain a deep knowledge of biomass pyrolysis in order to gain further understanding of the combustion and gasification processes (Sanchez-Silva et al., 2012). Kinetic analyses are useful for understanding the thermal degradation process and providing information for a pyrolysis process design using wood (Kim et al., 2010; Wongsiriamnuay and Tippayawong, 2010b). The kinetic modeling of the decomposition is crucial for an accurate prediction of the material's behavior under different working conditions (Sánchez-Jiménez et al., 2010). The pyrolysis of wood is a chemically complex process in which several reactions occur simultaneously. Because of this complexity, a large number of papers found in the literature assume different approaches to describe the thermal degradation of wood.

Órfão et al. (1999) introduced three independent reactions to describe the pyrolysis kinetics of some lignocellulosic materials, while Di Blasi (2008) used three parallel reactions to describe the fast pyrolysis process of wood. Yang et al. (2006) investigated the degradation of cellulose, hemicellulose and lignin separately to understand biomass pyrolysis. The authors proposed two steps of multiple linear-regression equations for predicting the component proportions in a biomass and the weight loss during pyrolysis.

Several kinetic equations for the description of solid state reactions such as random nucleation, nucleation and growth, diffusion and phase boundary controlled have been proposed (Criado et al., 1989) and used during the last decades (Núñez et al., 2000; Sánchez-Jiménez et al., 2010; Bianchi et al., 2011). When studying wood degradation reactions, many authors tend to ignore these models, adopting empirical first order or n-order models to describe the degradation process (Wu and Dollimore, 1998; Wongsiriamnuay and Tippayawong, 2010a,b; Kim et al., 2010; Luangkiattikhun et al., 2008; Shen et al., 2011) that have an inaccurate physical meaning and, even more important, give no guarantee if these are actually representative of the studied process (Sánchez-Jiménez et al., 2009). Therefore, this work focuses on determining the kinetic degradation mechanism that describes the decomposition process of four wood species from Brazil that are commonly used in the lumber industry. This understanding of the process will be realized through kinetic equations. It will enable an evaluation of how differences in wood composition and cellulose crystallinity influence the thermal degradation kinetics in wood.

### 1.1. Theoretical background

The fundamental equation used in all kinetic studies is generally described as Bianchi et al. (2011):

$$\frac{d\alpha}{dt} = k(T)f(\alpha) \quad (1)$$

where  $k$  is the rate constant and  $f(\alpha)$  is the reaction model, a function dependent on the reaction mechanism. Eq. 1 expresses the rate of conversion,  $d\alpha/dt$ , at a constant temperature as a function of the rate constant and the reduction in the reactant concentration. In this study, the conversion rate  $\alpha$  is defined as:

$$\alpha = \frac{m_0 - m_t}{m_0 - m_f} \quad (2)$$

where  $m_0$  is the initial weight of the sample,  $m_f$  is the final weight and  $m_t$  is the sample's weight at time ( $t$ ). The rate constant  $k$  is generally given by the Arrhenius equation:

$$k(T) = Ae^{-\frac{E_a}{RT}} \quad (3)$$

where  $E_a$  is the apparent activation energy ( $\text{kJ mol}^{-1}$ ),  $R$  is the gas constant ( $8.314 \text{ kJ mol}^{-1}$ ),  $A$  is the pre-exponential factor ( $\text{min}^{-1}$ ) and,  $T$  is the absolute temperature ( $K$ ). The combination of Eqs. (1) and (3) gives the following relationship:

$$\frac{d\alpha}{dt} = Ae^{-\frac{E_a}{RT}}f(\alpha) \quad (4)$$

For a dynamic thermogravimetric analysis (TGA) in a non-isothermal experiment, introducing the heating rate  $\beta = dT/dt$  into Eq. 4, Eq. 5 is obtained as:

$$\frac{d\alpha}{dT} = \left(\frac{A}{\beta}\right)e^{-\frac{E_a}{RT}}f(\alpha) \quad (5)$$

Eqs (4) and (5) are the fundamental expressions of analytical methods used to calculate kinetic parameters on the basis of the TGA data (Sánchez-Jiménez et al., 2010; Poletto et al., 2010; Shuping et al., 2010; Sanchez-Silva et al., 2012).

#### 1.1.1. Flynn–Wall–Ozawa method

The activation energy values for the degradation process were determined by the isoconversional Flynn–Wall–Ozawa (FWO) method. This method can be used for determination of the  $E_a$  values without any knowledge of the reaction mechanisms. This is defined by Eq. 6 (Flynn and Wall, 1966; Ozawa, 1965):

$$\log \beta = \log \left[ \frac{AE_a}{g(\alpha)R} \right] - 2.315 - 0.4567 \frac{E_a}{RT} \quad (6)$$

where  $\beta$  is the heating rate,  $A$  is the pre-exponential factor,  $g(\alpha)$  is a function of the conversion,  $E_a$  is the activation energy and  $R$  is the gas constant. Therefore, for different heating rates ( $\beta$ ) and a given degree of conversion ( $\alpha$ ), a linear relationship is observed by plotting  $\log \beta$  vs.  $1/T$ , and the  $E_a$  is obtained from the slope of the straight line (Flynn and Wall, 1966; Ozawa, 1965; Pistor et al., 2010).

**Table 1**

Algebraic expressions for  $g(\alpha)$  and  $f(\alpha)$  for the most frequently used mechanisms of solid state processes Criado et al. (1989), Núñez et al. (2000).

Mechanism – Solid state process	$g(\alpha)$	$f(\alpha)$
$A_2$ – Nucleation and growth (Avrami Eq. 1)	$[-\ln(1-\alpha)]^{1/2}$	$2(1-\alpha)[- \ln(1-\alpha)]^{1/2}$
$A_3$ – Nucleation and growth (Avrami Eq. 2)	$[-\ln(1-\alpha)]^{1/3}$	$3(1-\alpha)[- \ln(1-\alpha)]^{2/3}$
$A_4$ – Nucleation and growth (Avrami Eq. 3)	$[-\ln(1-\alpha)]^{1/4}$	$4(1-\alpha)[- \ln(1-\alpha)]^{3/4}$
$R_1$ – Phase boundary controlled reaction (one-dimensional movement)	$\alpha$	1
$R_2$ – Phase boundary controlled reaction (contracting area)	$[1-(1-\alpha)]^{1/2}$	$2(1-\alpha)^{1/2}$
$R_3$ – Phase boundary controlled reaction (contracting volume)	$[1-(1-\alpha)]^{1/3}$	$3(1-\alpha)^{2/3}$
$D_1$ – One-dimensional diffusion	$\alpha^2$	$(1/2)\alpha$
$D_2$ – Two-dimensional diffusion (Valensi equation)	$(1-\alpha)\ln(1-\alpha) + \alpha$	$[-\ln(1-\alpha)]^{-1}$
$D_3$ – Three-dimensional diffusion (Jander equation)	$[1-(1-\alpha)^{1/3}]^2$	$(3/2)[1-(1-\alpha)^{1/3}]^{-1}(1-\alpha)^{2/3}$
$D_4$ – Three-dimensional diffusion (Ginstling-Brounshtein equation)	$[1-(2/3)\alpha] - (1-\alpha)^{2/3}$	$(3/2)[1-(1-\alpha)^{1/3}]^{-1}$
$F_1$ – Random nucleation with one nucleus on the individual particle	$-\ln(1-\alpha)$	$1-\alpha$
$F_2$ – Random nucleation with two nuclei on the individual particle	$1/(1-\alpha)$	$(1-\alpha)^2$
$F_3$ – Random nucleation with three nuclei on the individual particle	$1/(1-\alpha)^2$	$(1/2)(1-\alpha)^3$



### 1.1.2. Criado method

The degradation reaction mechanism can be determined using the Criado method (Criado et al., 1989; Núñez et al., 2000), which can accurately determine the reaction mechanism in a solid reaction process. This is defined by a  $Z(\alpha)$  type function:

$$Z(\alpha) = \frac{(d\alpha/dt)}{\beta} \pi(x)T \quad (7)$$

where  $x = E_a/RT$  and  $\pi(x)$  is an approximation of the temperature integral that cannot be expressed in a simple analytical form. In this study, we used the fourth rational expression of Senum and Yang (Pérez-Maqueda and Criado, 2000), which gives errors of lower than  $10^{-5}\%$  when  $x > 20$ . The master curves as a function of the conversion degree corresponding to the different models listed in Table 1 (Bianchi et al., 2011; Shuping et al., 2010) were obtained according to Eq. 8:

$$Z(\alpha) = f(\alpha)g(\alpha) \quad (8)$$

From Eqs. (5) and (8), the following relationship can be derived:

$$Z(\alpha) = \frac{d\alpha}{dT} \frac{E_a}{R} \frac{\pi(x)}{e^{E_a/RT}} P(x) \quad (9)$$

Eq. (9) is used to represent the experimental curve. By comparing these two curves, the type of mechanism involved in the thermal degradation can be identified.

## 2. Methods

### 2.1. Materials

The wood flour samples used in this study were obtained from wastes of the Brazil lumber industry. The wood species investigated were *Pinus elliottii* (PIE), *Eucalyptus grandis* (EUG), *Mezilaurus itauba* (ITA) and *Dipteryx odorata* (DIP). Samples having a particle size of 200–300  $\mu\text{m}$  were dried in a vacuum oven at 105 °C for 24 h before the TGA. The wood moisture content before dried ranges between 4 and 6 wt.% (Poletto et al., 2011a). Wood composition and crystalline index (Cr.I.) are shown in Table 2 (Poletto et al., 2012).

### 2.2. Thermogravimetric analysis (TGA)

The thermogravimetric analysis (TGA50 – Shimadzu) was carried out under  $\text{N}_2$  atmosphere with a purge gas flow of 50  $\text{cm}^3 \cdot \text{min}^{-1}$  from 25 to 600 °C. Approximately 10 mg of each sample was used. The analysis was carried out at four different heating rates (5, 10, 20 and 40 °C  $\text{min}^{-1}$ ). The results obtained were used to calculate the kinetics parameters.

## 3. Results and discussions

### 3.1. Thermogravimetric analysis

The ITA wood shows a more significant weight loss than others wood species. For this wood the degradation process starts at around 180 °C, according to a previous work (Poletto et al., 2012). This behavior might be associated with the content of

extractives in this wood, approximately 14% as presented in Table 2, which is higher than the other wood samples. This results in degradation at lower temperatures (Shebani et al., 2008; Poletto et al., 2012). PIE and EUG begin the degradation process between 180 and 200 °C; they have more thermal stability than ITA probably because they contain a higher amount of cellulose and lignin and a lower quantity of extractives. However, the DIP wood that contains approximately 11% extractives showed the highest thermal stability in this range of temperature. DIP has the highest cellulose crystalline index, which probably slows the thermal decomposition of the wood.

When the  $\alpha$  values are between 0.1 and 0.2, the ITA sample has higher conversion values at lower temperatures, followed by EUG, DIP and PIE. The higher quantities of extractives in ITA may accelerate the degradation process and promote an increase in the conversion values at relatively low temperature. Extractives are compounds with low molecular mass (Gutiérrez et al., 1998; Mészáros et al., 2007) when compared with cellulose; they are formed by lipids, phenolic compounds, terpenoids, fatty acids, resin acids and waxes (Mészáros et al., 2007; Shebani et al., 2008) that promote the degradation of wood at relative lower temperatures as a result of their high volatility (Mészáros et al., 2007). The EUG sample has the second largest conversion in the low temperature range. EUG possesses higher quantities of adsorbed water and has prominent hemicellulose degradation at 250–300 °C that can lead to a higher conversion value at a lower temperature. In addition, the structure of lignin can help to interpret this result. The syringyl, as well as the guaiacyl units are built into the lignin macromolecule mainly by ether bonds, and the ether bonds between syringyl units are easier to split than those between guaiacyl units (Wang et al., 2009). This fact result in a higher thermal stability of softwood lignin mainly composed by guaiacyl units when compared with hardwood lignin composed by a mix of guaiacyl and syringyl units (Wang et al., 2009). So, the lowest thermal stability for EUG, a hardwood, and the highest thermal stability for PIE, a softwood, may also help to explain the higher thermal stability of this two wood samples when the conversion values are between 0.1 and 0.2, since according Table 2 PIE had the highest lignin content, followed by EUG. In contrast, the DIP and PIE species retain their lower conversion values as the temperature increases. Because DIP contains 11% extractives, the degradation process occurs slower than for the ITA sample that contains approximately 14% extractives; this is probably because the higher crystallinity of cellulose in DIP and a slower degradation of hemicelluloses. The PIE species, which contains less absorbed water than EUG, has the lowest conversion rate when temperature increases; PIE has a low content of extractives, the highest lignin content and a slower degradation of hemicellulose. To summarize, at low conversion values, the degradation process in wood seems to be mainly dominated by the following parameters, or some interrelationships between these parameters: the volatilization of water, the degradation of extractives, the degradation of lignin, the break-down of hemicelluloses, and the degradation of amorphous domains of cellulose.

When the conversion values are between 0.4 and 0.6, mainly the degradation of cellulose occurs. The wood species studied show a different thermal degradation behavior than when compared

**Table 2**  
Chemical composition and crystalline index of the wood species study.

Wood species	Holocellulose (%)	Lignin (%)	Extractives (%)	Ash (%)	Cr. I. (%)
<i>Eucalyptus grandis</i> (EUG)	62.7 ± 1.4	32.1 ± 1.0	4.1 ± 0.2	1.1 ± 0.3	34.4
<i>Pinus elliottii</i> (PIE)	61.2 ± 1.1	33.8 ± 1.0	4.5 ± 0.1	0.8 ± 0.1	34.1
<i>Dipteryx odorata</i> (DIP)	57.1 ± 0.6	30.4 ± 0.4	11.1 ± 0.1	1.5 ± 0.2	43.0
<i>Mezilaurus itauba</i> (ITA)	57.8 ± 1.0	28.0 ± 0.3	13.6 ± 0.7	0.7 ± 0.1	37.8

with low conversion values. Once again, ITA has the highest conversion values at low temperatures but is followed by PIE, EUG and DIP. In this range of conversion, the fast degradation process in ITA is probably influenced by the lower thermal stability of hemicellulose and the lower contents of holocellulose and lignin than other species studied. These factors lead to an acceleration of the degradation of cellulose because the degradation of one component may accelerate the degradation of the other wood components (Poletto et al., 2012). PIE and EUG possess comparable degradation profiles in this range of conversion, which may be associated with their similar chemical compositions and crystalline indices presented in Table 2. However, PIE has a slightly lower degradation value than EUG when the temperature increases. This slower cellulose degradation might be associated with the lower reactivity of hemicelluloses in PIE, which is a softwood species, than in EUG, which is a hardwood species. Grønli et al. (2002) observed that hemicellulose degradation is slower in softwoods than in hardwoods by studying softwoods from pine species and several hardwood species. The authors verified that hemicelluloses from softwood have a lower reactivity than hemicelluloses from hardwood, which is associated with the differences in chemical composition of the two species' hemicelluloses.

The DIP sample demonstrates the highest thermal stability throughout the second range of conversion evaluated. The organized cellulose chains in this wood may prevent the wood degradation given that the well-packed cellulose chains impede heat diffusion through the sample. The lower degradation of hemicellulose improves the thermal stability of DIP, even with substantial amounts of extractives. In summary, when the degradation occurs at low conversion values, the heat from heating source diffuses quickly in non-ordered regions and causes fast degradation of compounds with a low molecular mass. Alternatively, highly ordered cellulose regions may act as barriers to heat diffusion and impede the degradation of cellulose, increasing the wood's thermal stability. The rate of wood decomposition tends to increase when the heating rate also increases, because higher thermal energy was provided to the sample which causes better heat transfer between the surrounding and inside the samples (Wongsiriamnuay and Tippayawong, 2010a). However, external diffusion effects or heat or mass transfer limitations for the samples may also occur.

### 3.2. Kinetics results

The plots of the FWO method, which was used for the determination of the  $E_a$  values for all species studied, show a general trend. Because the kinetic behavior is similar for all of the wood species studied, only ITA was chosen as a representative model for the presentation of the  $E_a$  results. Therefore, Fig. 1 shows the results of the application of the FWO method with  $\alpha$  values from 0.1 to 0.8. The linear fits obtained from the plot of  $\log \beta$  vs.  $1/T$  are also shown in Fig. 2. The  $E_a$  values were calculated from the angular coefficient obtained from the straight line fit. Table 3 summarizes the  $E_a$  values for all of the wood samples studied.

As seen in Table 3, when  $\alpha = 0.1$ , the  $E_a$  values are approximately  $185 \text{ kJ mol}^{-1}$  for the EUG and PIE species that contain lower quantities of extractives. They are approximately  $175 \text{ kJ mol}^{-1}$  for the ITA and DIP species that contain higher extractive contents. These results confirm the fact that the extractives promote the degradation of wood at relatively low temperatures, reducing the thermal stability of wood. When the conversion is 0.2, all wood species studied have an  $E_a$  of nearly  $200 \text{ kJ mol}^{-1}$ . The slight increase in the  $E_a$  values of the wood samples when  $\alpha > 0.2$  implies the possible occurrence of a decomposition process of the main components (Yao et al., 2008). When  $\alpha = 0.2$  the temperature lies at around  $300 \text{ }^\circ\text{C}$ , which is indicative that the degradation process begins to occur in the hemicelluloses and in the amorphous domains of

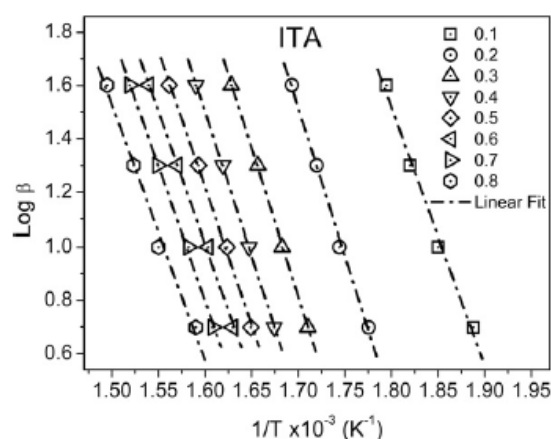


Fig. 1. Plot of FWO method for ITA wood showing the linear fits obtained.

the cellulose leading to an increase of the  $E_a$  values. According to Mamliev et al. (2006) the depolymerization of cellulose by transglycosylation during pyrolysis involves an activation energy close to  $200 \text{ kJ mol}^{-1}$ . ITA and PIE have  $E_a$  values close to  $200 \text{ kJ mol}^{-1}$  only at conversion values of 0.2–0.3. This indicates that they have a lower thermal stability than EUG and DIP probably because they contain lower quantities of cellulose and a lower crystallinity index, respectively. However, the  $E_a$  values for EUG and DIP were approximately  $200 \text{ kJ mol}^{-1}$  during all conversion values evaluated. EUG has the highest quantities of holocellulose and lignin, which leads to higher  $E_a$  values. DIP has ordered cellulose regions that retard the degradation process, leading to a higher  $E_a$  as the temperature increases.

The  $E_a$  values obtained using the FWO method were used to determine the thermal degradation mechanisms proposed by Criado et al. (1989), since according to FWO method the activation energy can be determined without any knowledge of the reaction mechanisms and then these values were used in Criado method. This method uses reference theoretical curves obtained from Eq. 8 that are derivatives of the  $f(\alpha)$  and  $g(\alpha)$  functions represented in Table 1; called master curves, they are compared to experimental data to determine the mechanism of the solid-state degradation process (Criado et al., 1989; Sánchez-Jiménez et al., 2009). As seen in Table 1, the algebraic expressions that represent the theoretical mechanisms are separated into four groups:  $A_n$ ,  $R_n$ ,  $D_n$  and  $F_n$ . Respectively, these mechanisms describe: nuclei formation processes for the propagation of thermal degradation; diffusion processes that are related to the heat transfer capacity along the material structure; reaction mechanisms controlled by the surface of the sample; and the random degradation of nuclei. The determination of the  $Z(\alpha)$  values was carried out using a heating rate ( $\beta$ ) of  $10 \text{ }^\circ\text{C min}^{-1}$ , and the calculated  $Z(\alpha)$  values were determined by applying the  $E_a$  values obtained with the FWO method to Eq. 9. Fig. 2 presents the master curves as well as the results of the experimental data obtained.

The experimental data in Fig. 2 shows that for all wood species studied in the range of  $\alpha = 0.2$ – $0.4$ , they overlap the D1, D2 and D3 curves. According to literature, these degradation mechanisms refer to a diffusion process in one, two and three dimensions, respectively (Criado et al., 1989). Similar results were described by Wu and Dollimore (1998), Bianchi et al. (2010) and Poletto et al. (2011b) for other cellulosic fibers. Based on this result, at lower conversion values, the heating transfer occurs by diffusion throughout the sample. However, the higher thermal stability of DIP may be related to a difficulty in the heat transfer process because of the higher-ordered cellulose regions. When the conver-



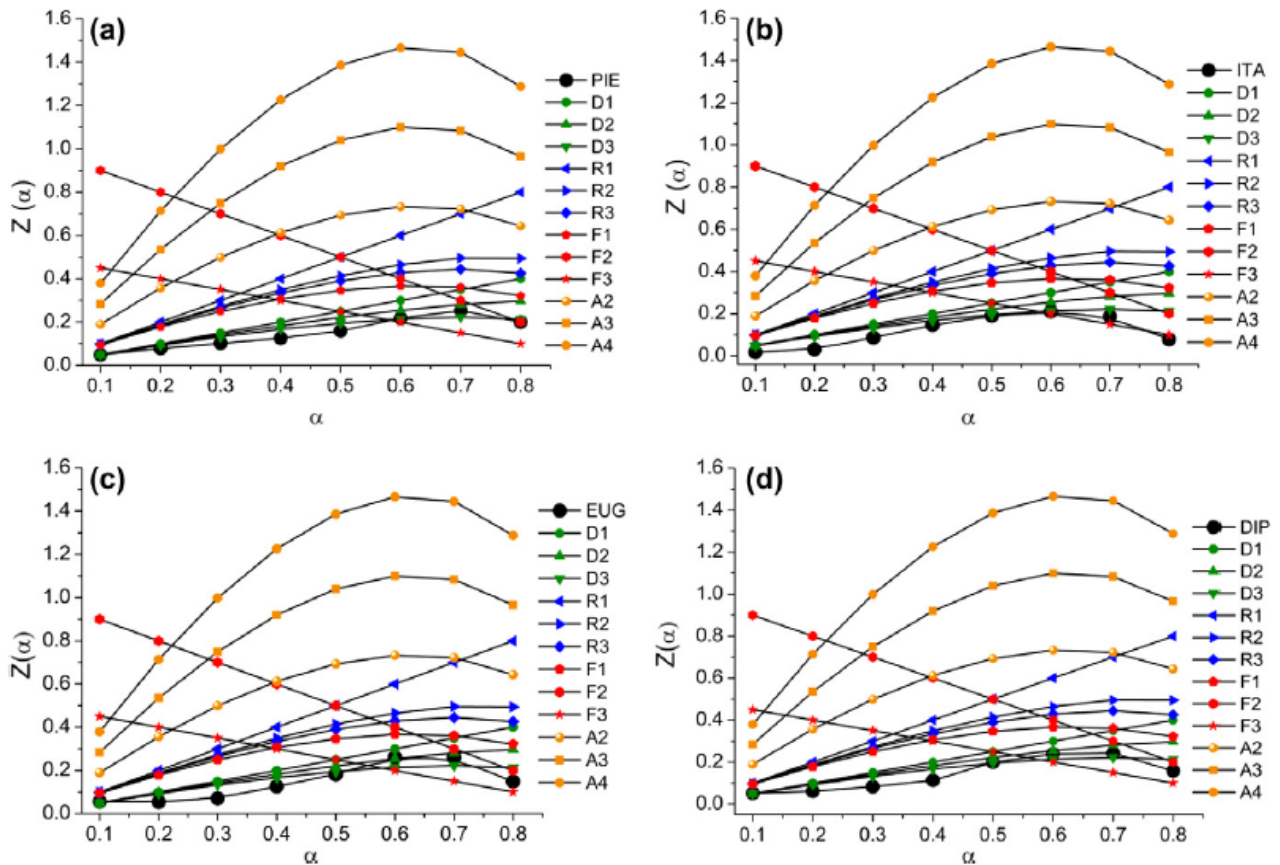


Fig. 2. Master curves and experimental data obtained using the Criado method for PIE (a), ITA (b), EUG (c) and DIP (d).

**Table 3**  
Activation energies obtained using the FWO method for the wood species studied.

$\alpha$	EUG		PIE		DIP		ITA	
	$E_a$ (kJ mol <sup>-1</sup> )	$R$	$E_a$ (kJ mol <sup>-1</sup> )	$R$	$E_a$ (kJ mol <sup>-1</sup> )	$R$	$E_a$ (kJ mol <sup>-1</sup> )	$R$
0.1	184.9	-0.995	183.2	-0.992	174.8	-0.999	175.1	-0.996
0.2	205.0	-0.998	210.3	-0.995	196.3	-0.996	200.6	-0.998
0.3	229.7	-0.998	202.5	-0.995	211.9	-0.996	200.5	-0.999
0.4	221.1	-0.999	194.7	-0.997	213.7	-0.998	195.7	-0.999
0.5	218.3	-0.998	191.2	-0.999	206.3	-0.999	186.0	-0.998
0.6	198.6	-0.999	186.6	-0.999	199.3	-0.999	180.2	-0.999
0.7	195.4	-0.999	179.6	-0.999	192.8	-0.999	182.0	-0.999
0.8	208.5	-0.999	180.8	-0.999	206.4	-0.997	173.8	-0.996

sion values are higher than 0.5, the degradation mechanism for PIE, EUG and DIP species tends towards F1, which corresponds to random nucleation with one nucleus in the individual particle (Criado et al., 1989). In this type of mechanism, the degradation is initiated from random points that act as growth center for the development of the degradation reaction. Based on this, at conversion values above 0.5, the higher temperatures involved in the degradation process at approximately 350 °C may promote the rupture of some ordered cellulose chains. These low molecular mass chains can possibly act as centers for random nucleation and growth for the degradation reaction. The amorphous cellulose domains also can probably act as a center for degradation and stimulate the degradation process. Its degradation occurs in lower conversion ranges when the heat is propagated throughout the sample, as discussed above.

The shape of the experimental curve for ITA is similar to the curves for the other species. However, the Z values overlap the

D<sub>3</sub> mechanism, associated with the diffusion process in three dimensions. This behavior may be associated with the highest degradation of the extractives and the hemicellulose content that can lead to a higher volatility of the main wood components at relatively low temperatures. This can probably promote an acceleration of the cellulose degradation by diffusion, not only by the diffusion of the heat from heating source but also by diffusion of the hot gasses formed throughout the sample. The same mechanism for wood was observed by Wang et al. (2006).

#### 4. Conclusions

The thermal degradation of wood is influenced by its composition and crystallinity. Higher extractive contents accelerate the degradation process, promoting an increase of conversion values at low temperatures. Higher reactivity of hemicelluloses and lignin

can accelerate the degradation reaction and cause cellulose degradation at low temperatures. Organized cellulose regions may prevent wood degradation; well-packed cellulose chains impede the heat diffusion, promoting a slower degradation process. Wood degradation is governed by diffusion when the conversion values are below 0.4 and tends to random nucleation, a F1 mechanism, when the conversion values are above 0.5.

### Acknowledgements

The authors are grateful to Prof. Ricardo Campomanes from Universidade Federal de Mato Grosso for supplying the DIP and ITA wood samples and Coordenação de Aperfeiçoamento de Pessoal de Nível Superior (CAPES) for financial support.

### References

- Bianchi, O., Dal Castel, C., de Oliveira, R.V.B., Bertuoli, P.T., Hillig, É., 2010. Nonisothermal degradation of wood using thermogravimetric measurements. *Polímeros* 20, 395–400.
- Bianchi, O., Martins, J.DeN., Florio, R., Oliveira, R.V.B., Canto, L.B., 2011. Changes in activation energy and kinetic mechanism during EVA crosslinking. *Polym. Test.* 30, 616–624.
- Criado, J.M., Málek, J., Ortega, A., 1989. Applicability of the master plots in kinetic analysis of non-isothermal data. *Thermochim. Acta* 147, 377–385.
- Di Blasi, C., 2008. Modeling chemical and physical process of wood and biomass pyrolysis. *Prog. Energy Combust. Sci.* 34, 47–90.
- Flynn, J.H., Wall, L.A., 1966. General treatment of the thermogravimetry of polymers. *J. Res.Nat. Bureau Stand.* 70A, 487–523.
- Gutiérrez, A., del Rio, J.C., González-Villa, F.J., Martín, F., 1998. Analysis of lipophilic extractives from wood and pitch deposits by solid phase extraction and gas chromatography. *J. Chromatogr. A* 823, 449–455.
- Grønli, M.G., Várhegyi, G., Di Blasi, C., 2002. Thermogravimetric analysis and devolatilization kinetics of wood. *Ind. Eng. Chem. Res.* 41, 4201–4208.
- Kim, S.-S., Kim, J., Park, Y.-H., Park, Y.-K., 2010. Pyrolysis kinetics and decomposition characteristics of pine trees. *Bioresour. Technol.* 101, 9797–9802.
- Luangkiattikhun, P., Tangsathikulchai, C., Tangsathikulchai, M., 2008. Non-isothermal thermogravimetric analysis of oil-palm solid wastes. *Bioresour. Technol.* 99, 986–997.
- Mamleev, V., Bourbigot, S., Le Bras, M., Yvon, J., Lefebvre, J., 2006. Model-free method for evaluation of activation energies in modulated thermogravimetry and analysis of cellulose decomposition. *Chem. Eng. Sci.* 61, 1276–1292.
- Mészáros, E., Jakab, E., Várhegyi, G., 2007. TG/MS, PyGC/MS and THM-GC/MS study of the composition and thermal behavior of extractive components of *Robinia pseudoacacia*. *J. Anal. Appl. Pyrolysis* 98, 61–70.
- Núñez, L., Fraga, F., Núñez, M.R., Villanueva, M., 2000. Thermogravimetric study of the decomposition process of the system BADGE (n = 0)/1,2 DCH. *Polymer* 41, 4635–4641.
- Órfão, J.J.M., Antunes, F.J.A., Figueiredo, J.L., 1999. Pyrolysis kinetics of lignocellulosic materials – three independent reactions model. *Fuel* 78, 349–358.
- Ozawa, T., 1965. A new method of analyzing thermogravimetric data. *Bull. Chemical Soc. Jap.* 38, 1881–1886.
- Pérez-Maqueda, L.A., Criado, J.M., 2000. The accuracy of Senum and Yang's approximations to the Arrhenius integral. *J. Therm. Anal. Calorim.* 60, 909–915.
- Pistor, V., Ornaghi, F.G., Ornaghi Jr., H.L., Florio, R., Zattera, A.J., 2010. Thermal characterization of oil extracted from ethylene-propylene-diene terpolymer residues (EPDM-r). *Thermochim. Acta* 510, 93–96.
- Poletto, M., Dettenborn, J., Pistor, V., Zeni, M., Zattera, A.J., 2010. Materials produced from plant biomass. Part I: evaluation of thermal stability and pyrolysis of wood. *Mater. Res.* 13, 375–379.
- Poletto, M., Zattera, A.J., Forte, M.M.C., Santana, R.M.C., 2011a. Influence of extractive content on wood flour thermal stability of different wood species from Brazil. 27th World Congress of the Polymer Processing Society (PPS-27), Morocco.
- Poletto, M., Pistor, V., Zeni, M., Zattera, A.J., 2011b. Crystalline properties and decomposition kinetics of cellulose fibers in wood pulp obtained by two pulping process. *Polym. Degrad. Stab.* 96, 679–685.
- Poletto, M., Zattera, A.J., Forte, M.M.C., Santana, R.M.C., 2012. Thermal decomposition of wood: influence of wood components and cellulose crystallite size. *Bioresour. Technol.* 109, 148–153.
- Popescu, M.-C., Popescu, C.-M., Lisa, G., Sakata, Y., 2011. Evaluation of morphological and chemical aspects of different wood species by spectroscopy and thermal methods. *J. Mol. Struct.* 988, 65–72.
- Sánchez-Jiménez, P.E., Pérez-Maqueda, L.A., Perejón, A., Criado, J.M., 2010. A new model for the kinetic analysis of thermal degradation of polymers driven by random scission. *Polym. Degrad. Stab.* 95, 733–739.
- Sánchez-Jiménez, P.E., Pérez-Maqueda, L.A., Perejón, A., Criado, J.M., 2009. Combined kinetic analysis of thermal degradation of polymeric materials under any thermal pathway. *Polym. Degrad. Stab.* 94, 2079–2085.
- Sanchez-Silva, L., López-González, D., Villaseñor, J., Sánchez, P., Valverde, J.L., 2012. Thermogravimetric-mass spectrometric analysis of lignocellulosic and marine biomass pyrolysis. *Bioresour. Technol.* 109, 163–172.
- Shebani, A.N., van Reenen, A.J., Meincken, M., 2008. The effect of wood extractives on the thermal stability of different wood species. *Thermochim. Acta* 471, 43–50.
- Shen, D.K., Gu, S., Jin, B., Fang, M.X., 2011. Thermal degradation mechanisms of wood under inert and oxidative environments using DAEM methods. *Bioresour. Technol.* 102, 2047–2052.
- Shuping, Z., Yulong, W., Mingde, Y., Chun, L., Jumao, T., 2010. Pyrolysis characteristics and kinetics of the marine microalgae *Dunaliella tertiolecta* using thermogravimetric analyzer. *Bioresour. Technol.* 101, 359–365.
- Yang, H., Yan, R., Chen, H., Zheng, C., Lee, D.H., Liang, D.T., 2006. In-depth investigation of biomass pyrolysis based on three major components: hemicellulose, cellulose and lignin. *Energy Fuels* 20, 388–393.
- Yao, F., Wu, Q., Lei, Y., Guo, W., Xu, Y., 2008. Thermal decomposition kinetics of natural fibers: activation energy with dynamic thermogravimetric analysis. *Polym. Degrad. Stab.* 93, 90–98.
- Wang, J., Wang, G., Zhang, M., Chen, M., Li, D., Min, F., Chen, M., Zhang, S., Ren, Z., Yan, Y., 2006. A comparative study of thermolysis characterization and kinetics of seaweeds and fir wood. *Process Biochem.* 41, 1883–1886.
- Wang, S., Wang, K., Liu, Q., Gu, Y., Luo, Z., Cen, K., Frasson, T., 2009. Comparison of the pyrolysis behavior of lignins from different tree species. *Biotechnol. Adv.* 27, 562–567.
- Wongsiriamnuay, T., Tippayawong, N., 2010a. Thermogravimetric analysis of giant sensitive plants under air atmosphere. *Bioresour. Technol.* 101, 9314–9320.
- Wongsiriamnuay, T., Tippayawong, N., 2010b. Non-isothermal pyrolysis characteristics of giant sensitive plants using thermogravimetric analysis. *Bioresour. Technol.* 101, 5638–5644.
- Wu, Y., Dollimore, D., 1998. Kinetic studies of thermal degradation of natural cellulosic materials. *Thermochim. Acta* 324, 49–57.



## 5 DISCUSSÃO E INTEGRAÇÃO DOS ARTIGOS

No Artigo I e também no Artigo II observa-se que as espécies de madeira estudadas possuem diferenças significativas em sua composição química. As espécies EUG e PIE apresentaram teores de holocelulose e lignina superiores ao das espécies DIP e ITA. Por outro lado, as espécies oriundas da região amazônica possuem teor de extrativos, em média, três vezes maior que as espécies provenientes da Serra Gaúcha.

Estas diferenças ficaram evidentes nos espectros de FTIR apresentados no Artigo I. A espécie ITA apresentou bandas mais proeminentes que as outras espécies estudadas a  $2916$  e  $2852\text{ cm}^{-1}$ . Estas bandas são características de grupos metila e metilênicos [37-38] e podem ser atribuídas aos extrativos. Para a espécie ITA os extrativos podem ser formados por compostos orgânicos como ésteres de ácidos graxos, como mostrado na Tabela 1, e assim possuem grupos  $\text{CH}_3$  e  $\text{CH}_2$  em sua constituição. A espécie EUG apresentou a banda em  $1736\text{ cm}^{-1}$  com maior intensidade que as outras espécies de madeira. Esta banda é associada ao estiramento da carbonila presente na hemicelulose [37-38]. Este resultado está de acordo com a maior quantidade de holocelulose observada para a EUG em comparação as demais espécies conforme apresentado nos Artigos I e II.

A determinação da energia envolvida nas ligações hidrogênio intramoleculares entre os grupos fenólicos da lignina em  $3567\text{ cm}^{-1}$  e também das ligações intramoleculares da celulose em  $3432\text{ cm}^{-1}$ , calculadas no Artigo I, bem como aquelas características da celulose cristalina em aproximadamente  $3278\text{ cm}^{-1}$  e  $3221\text{ cm}^{-1}$  mostraram que, em geral, as espécies DIP e ITA apresentaram maiores energias de ligação com menor distância entre as ligações hidrogênio, que as espécies EUG e PIE. Este resultado indica que provavelmente para as espécies DIP e ITA as cadeias de celulose estão mais fortemente unidas por ligações hidrogênio formando uma estrutura mais densamente empacotada e organizada que nas espécies EUG e PIE. Os resultados do índice de cristalinidade, discutidos no Artigo II, confirmam que as espécies DIP e ITA possuem maior quantidade de celulose cristalina que a EUG e PIE. É interessante observar também que o tamanho dos cristalitos, de maneira geral, também é superior nas espécies DIP e ITA. A maior

organização das cadeias de celulose nestas duas espécies faz com que as regiões de celulose amorfa sejam reduzidas o que por sua vez resulta em aumento do tamanho dos cristalitos e conseqüentemente do índice de cristalinidade.

A fração de cadeias de celulose contidas no interior dos cristalitos, denotada por X [37], também é superior nas espécies DIP e ITA que na EUG e PIE, conforme pode ser observado no Artigo II. Este resultado também vem ao encontro da maior energia de ligação hidrogênio e menor distância entre as ligações hidrogênio verificada no Artigo I. As espécies DIP e ITA contêm uma maior quantidade de cadeias de celulose em uma forma mais organizada no interior de seus cristalitos que as espécies EUG e PIE. Este comportamento pode acarretar em uma maior quantidade de ligações hidrogênio com maior energia entre cadeias de celulose vizinhas devido a sua maior proximidade o que resulta em uma celulose mais densamente empacotada o que por sua vez acarreta o maior índice de cristalinidade observado para as espécies DIP e ITA.

Os valores de Índice de Cristalinidade Total (TCI) e Índice de Ordenamento Lateral (LOI) associados à cristalinidade da celulose calculados a partir de relações entre bandas no espectro de FTIR no Artigo I não mostraram correlação com os resultados da análise de difração de raios X, apresentadas no Artigo II. Os valores de TCI foram superiores para as amostras EUG e PIE em comparação as amostras de DIP e ITA. Enquanto, que os valores de LOI foram maiores para a EUG seguida das espécies DIP, PIE e ITA, respectivamente. Os valores de TCI para as amostras ITA e DIP podem ter sido afetados pela maior quantidade de extrativos nestas duas espécies [36], uma vez que, os valores de TCI são obtidos pela relação entre a altura das bandas em aproximadamente  $1370\text{ cm}^{-1}$  e  $2900\text{ cm}^{-1}$ . Como discutido anteriormente, as espécies ITA e DIP possuem maior quantidade de extrativos que as espécies EUG e PIE, o que pode acarretar na redução dos valores de TCI para as espécies oriundas da região amazônica. Da mesma forma, os valores de LOI podem também ter sido afetados por outros componentes da madeira e assim, não apresentar correlação com os resultados de cristalinidade obtidos da análise de difração de raios X. Os valores de Intensidade de Ligação Hidrogênio (HBI), que podem ser relacionados com a cristalinidade da celulose, obtidos da relação entre os valores de absorvância

em  $3400\text{ cm}^{-1}$  e  $1320\text{ cm}^{-1}$ , respectivamente, também não apresentaram correlação com os resultados de difração de raios X. Deve-se considerar que os valores de absorbância em  $3400\text{ cm}^{-1}$  além de estarem relacionados com a celulose [37-38] podem também representar uma quantidade de água presente na amostra, tanto proveniente de umidade quanto de água de constituição da madeira. Assim, se na amostra de madeira estiver contida umidade ou uma maior quantidade de água de constituição os valores de HBI não irão representar diretamente a cristalinidade da celulose presente na amostra de madeira.

As análises termogravimétricas, apresentadas nos Artigos I e II, demonstraram que a espécie ITA, que possui aproximadamente 14% de extrativos, apresentou a menor estabilidade térmica frente a todas as madeiras estudadas. Este comportamento pode estar relacionado à baixa estabilidade térmica dos extrativos nesta espécie o que pode acarretar em redução da estabilidade térmica da madeira. No entanto, a espécie DIP, que contém 11% de extrativos, mostrou maior estabilidade térmica que a ITA. Este resultado pode estar associado ao maior índice de cristalinidade e maior tamanho de cristalito presente na DIP em comparação a ITA. Quando se compara as espécies com menor teor de extrativos observa-se que a espécie PIE apresentou maior estabilidade térmica que a EUG. A espécie EUG apresentou a maior perda de massa a baixas temperaturas, cerca de 2% em  $100^{\circ}\text{C}$ , associada à maior quantidade de água presente nesta espécie em comparação a PIE. Com base nos resultados obtidos no Artigo III, pode-se inferir que a baixas conversões, entre 10-30%, a degradação térmica da madeira parece estar relacionada com a volatilização da água, a degradação dos extrativos, o início da degradação da lignina e da hemicelulose e por fim a degradação das regiões amorfas da celulose.

O maior processo de degradação térmica tanto da hemicelulose quanto da celulose ocorre quando os valores de conversão atingem 40-60%. Neste estágio as amostras PIE e EUG apresentam comportamento semelhante, uma vez que, possuem tanto composição química quanto índices de cristalinidade semelhantes. Para a espécie ITA a degradação foi mais acelerada nesta faixa de conversão em comparação as demais espécies. O rápido processo de degradação da ITA pode estar associado à baixa estabilidade térmica das

hemiceluloses presentes nesta espécie, como também devido a degradação dos extrativos que pode acelerar a degradação da hemicelulose e também da celulose. Por outro lado, a espécie DIP apresentou maior estabilidade térmica que as demais espécies. A maior quantidade de celulose cristalina nesta madeira pode prevenir a sua degradação, já que a maior organização das cadeias de celulose resulta em maior empacotamento das cadeias e pode impedir a difusão através da amostra o que aumenta a estabilidade térmica. A baixa degradação da hemicelulose, mesmo com uma quantidade elevada de extrativos também contribui para a elevada estabilidade térmica desta espécie frente às demais madeiras estudadas.

Em resumo, quando o processo de degradação ocorre em baixos valores de conversão, o calor é transferido rapidamente pelas regiões não ordenadas da amostra causando a rápida degradação dos componentes de baixa massa molecular. No entanto, as regiões de elevada ordenação, como as regiões ricas em celulose ordenada, podem atuar como barreiras a esta transferência e impedir a degradação da celulose e como resultado a estabilidade térmica da madeira aumenta.

Os valores de energia de ativação, discutidos no Artigo III, mostraram que quando a conversão é igual a 10% a energia de ativação das espécies EUG e PIE é 10 kJ/mol superior as amostras com maiores teores de extrativos. Este comportamento corrobora o fato de que os extrativos promovem a degradação da madeira a baixas temperaturas. A energia de ativação parece não ser afetada tanto pela cristalinidade da celulose quanto pelo tamanho dos cristalitos. Kim et al., [49] também obtiveram resultados semelhantes em diversas amostras de celulose. Para os outros valores de conversão avaliados a energia de ativação para todas as espécies estudadas variou em torno de 180 a 220 kJ/mol.

As espécies estudadas apresentaram mecanismo de degradação por difusão ( $D_n$ ) entre 10-40% de conversão. Este mecanismo refere-se ao processo de difusão em uma, duas e três dimensões. De acordo com este resultado, em baixas conversões os processos de difusão ocorrem através da amostra. Em valores de conversão próximos a 50% o mecanismo de degradação para as espécies DIP, PIE e EUG tende para F1, ou seja, correspondente a uma degradação por nucleação aleatória. Este mecanismo

representa uma degradação iniciada em pontos aleatórios que atuam como centros de crescimento para o desenvolvimento das reações de degradação. Para a amostra ITA o comportamento da curva experimental é similar ao das outras espécies. No entanto, os valores experimentais sobrepõem os valores do mecanismo D3, associado ao processo de difusão em três dimensões, ao longo da conversão. Este comportamento pode estar associado com a maior degradação dos extrativos que podem acarretar na aceleração da degradação da hemicelulose proporcionando elevada volatilização da madeira a baixas temperaturas. Como resultado, a degradação da celulose por difusão pode ser acelerada e ocorrer não somente pela transferência do calor através da amostra, mas também pela transferência dos gases formados pela volatilização dos extrativos.

## 6 CONCLUSÃO

Em suma os resultados demonstraram que a degradação térmica da madeira é influenciada pela sua composição e também pela cristalinidade da celulose presente em cada espécie. Os elevados teores de extrativos, em geral, aceleram o processo de degradação térmica da madeira e quando são associados à rápida degradação da hemicelulose e lignina e podem resultar na degradação da celulose em baixas temperaturas. Por outro lado, regiões de celulose com elevado ordenamento podem retardar a degradação da madeira, uma vez que a maior organização da celulose impede a difusão do calor pela amostra o que resulta em madeiras com maior estabilidade térmica.

A determinação da energia envolvida nas ligações hidrogênio intramoleculares da lignina e também da celulose mostrou correlação com a cristalinidade obtida pela análise de raios X. No entanto, os valores de LOI, TCI e HBI, associados à cristalinidade da celulose e obtidos pelas análises de FTIR não apresentam relação com a cristalinidade da celulose obtida pela análise de raios X, provavelmente devido à influência da umidade, dos extrativos e dos demais componentes da madeira.

Assim, os resultados obtidos indicaram que além dos extrativos, o tamanho dos cristalitos e a cristalinidade da celulose também influenciam o processo de degradação da madeira. A energia de ativação demonstrou não ser afetada pela cristalinidade e pelo tamanho do cristalito da celulose. O processo de degradação térmica da madeira ocorre através de mecanismos de difusão até valores de conversão próximos de 40% e então quando os valores de conversão para as amostras DIP, EUG e PIE atingem valores acima de 50% estas espécies tendem a mecanismos de degradação F1 provavelmente devido à ruptura de algumas cadeias de celulose originando cadeias de menor massa molar que podem atuar como centros para reações de degradação aleatórias. A degradação térmica da espécie ITA não seguiu esta tendência indicando que os extrativos podem influenciar na degradação da madeira acelerando o processo de degradação dos demais componentes por processo de difusão tanto pela transferência do calor quanto pela volatilização destes compostos de baixa massa molecular.

## **7 SUGESTÕES PARA TRABALHOS FUTUROS**

A partir dos resultados obtidos neste trabalho fazem-se algumas sugestões para a realização de trabalhos futuros, como:

- Remover os extrativos das espécies de madeira estudadas e avaliar o efeito desta remoção na estabilidade térmica e na cinética de degradação das quatro espécies;
- Desenvolver compósitos termoplásticos utilizando as espécies de madeira com e sem extrativos e avaliar as propriedades térmicas e mecânicas dos compósitos.

## 8 REFERÊNCIAS

- [1] DAIAN, G.; OZARSKA, B. Wood waste management practices and strategies to increase sustainability standards in the Australian wooden furniture manufacturing sector. **Journal of Cleaner Production**. Vol. 17, p. 1594-1602, 2009.
- [2] ESHUN, J. F.; POTTING, J.; LEEMANS, R. Wood waste minimization in the timber sector of Ghana: a systems approach to reduce environmental impact. **Journal of Cleaner Production**. Vol. 26, p. 67-78, 2012.
- [3] DERCAN, B.; LUKÍC, T.; BUBALO-ZIVKOVÍC, M.; DURDEV, B.; STOJSAVLJEVIĆ, R.; PANTELÍC, M. Possibility of efficient utilization of wood waste as a renewable energy resource in Serbia. **Renewable and Sustainable Energy Reviews**. Vol. 16, p. 1516-1527, 2012.
- [4] MASSOTE, C.H.R.; SANTI, A.M.M. Implementation of a cleaner production program in a Brazilian wooden furniture factory. **Journal of Cleaner Production**. Vol. 46, p. 89-97, 2013.
- [5] GONÇALVES, M.T.T. Processamento da madeira. Bauru: M.T.T. Gonçalves, 2000.
- [6] BRAND, M.A.; KLOCK, U.; MUÑIZ, G.I.B.; SILVA, D.A. Avaliação do processo produtivo de uma indústria de manufatura de painéis por meio do balanço de materiais e do rendimento da matéria-prima. **Revista Árvore**. Vol 28, p. 553-562, 2004.
- [7] SCHNEIDER, V.E.; HILLIG, É.; WEBER, C. Situação ambiental da indústria madeireira – caracterização e aproveitamento dos resíduos. In: Congresso Brasileiro de Engenharia Sanitária e Ambiental, 24, Belo Horizonte. **Anais...** Belo Horizonte, 2004.



[8] HILLIG, É.; SCHNEIDER, V.E.; WEBER, C.; TECCHIO, R.D. Resíduos de madeira da indústria madeireira – caracterização e aproveitamento. In: Encontro Nacional de Engenharia de Produção, 26, Fortaleza. **Anais...** Fortaleza, 2006.

[9] SCHNEIDER, V.E.; HILLIG, É.; BERTOTTO FILHO, L.A.; RIZZON, M.R. Geração de resíduos de madeira e derivados no pólo moveleiro da Serra Gaúcha – diagnóstico e indicativos para o gerenciamento ambiental na indústria moveleira. In: Simpósio Luso-Brasileiro de Engenharia Sanitária e Ambiental, 11, Rio Grande do Norte. **Anais...** Rio Grande do Norte, 2004.

[10] HILLIG, É.; SCHNEIDER, V.E.; PAVONI, E.T. Pólo moveleiro da Serra Gaúcha: geração de resíduos e perspectivas para sistemas de gerenciamento ambiental. Caxias do Sul: Educs, 2004.

[11] SCHNEIDER, V.E.; NEHME, M.C.; BEN, F. Pólo moveleiro da Serra Gaúcha: sistemas de gerenciamento ambiental na indústria moveleira. Caxias do Sul: Educs, 2006.

[12] BLEDZKI, A.K.; MAMUN, A.; VOLK, J. Barley husk and coconut shell reinforced polypropylene composites: the effect of fibre physical, chemical and surface properties. **Composites Science and Technology**. Vol. 70, p. 840-846, 2010.

[13] LA MANTIA, F.P.; MORREALE, M. Green composites: a brief review. **Composites Part A**, Vol. 42, p. 579-588, 2011.

[14] NOURBAKHSI, A.; ASHORI, A. Wood plastic composites from agro-waste materials: analysis of mechanical properties. **Bioresource Technology**, Vol. 101, p. 2525-2528, 2010.

[15] FÁVARO, S.L.; LOPES, M.S.; NETO, A.G.V.C.; SANTANA, R.R.; RADOVANOVIC, E. Chemical, morphological, and mechanical analysis of rice

husk/post-consumer polyethylene composites. **Composites Part A**, Vol. 41, p. 154-160, 2010.

[16] POLETTI, M.; ZENI, M.; ZATTERA, A.J. Effects of wood flour addition and coupling agent content on mechanical properties of recycled polystyrene/wood flour composites. **Journal of Thermoplastic Composite Materials**. Vol.25, p. 821-833, 2012.

[17] POLETTI, M.; DETTENBORN, J.; ZENI, M.; ZATTERA, A.J. Characterization of composites based on expanded polystyrene wastes and wood flour. **Waste Management**, Vol.31, p. 779-784, 2011.

[18] ISLAM, M.N.; RAHMAN, M.R.; HAQUE, M.M.; HUQUE, M.M. Physico-mechanical properties of chemically treated coir reinforced polypropylene composites. **Composites Part A**, Vol.41, p. 192-198, 2010.

[19] SLIWA, F.; EL-BOUNIA, N.; CHARRIER, F.; MARIN, G.; MALET, F. Mechanical and interfacial properties of wood and bio-based thermoplastic composite. **Composites Science and Technology**. Vol 72, p. 1733-1740, 2012.

[20] GEORGE, G.; JOSEPH, K.; NAGARAJAN, E.R.; TOMLAL JOSE, E.; SKRIFVARS, M. Thermal, calorimetric and crystallization behaviour of polypropylene/jute yarn bio-composites fabricated by commingling technique. **Composites Part A**, Vol.48, p. 110-120, 2013.

[21] ROWELL, R.M. Wood chemistry and wood composites. Boca Raton: CRC Press, 2005.

[22] JOHN, M.J.; SABU THOMAS. Biofibres and biocomposites. **Carbohydrate Polymers**. Vol 71, p. 343-364, 2008.

[23] HON, D.N.S. Wood and cellulosic chemistry. New York: Marcel Dekker, 2000.

- [24] AKERHOL, M.; HINTERSTOISSER, B.; SALMEN, L. Characterization of the crystalline structure of cellulose using static and dynamic FT-IR spectroscopy. **Carbohydrate Research**. Vol 339, p. 569-578, 2004.
- [25] BLEDZKI, A.K.; GASSAN, J. Composites reinforced with cellulose based fibres. **Progress in Polymer Science**. Vol 24, p. 221-274, 1999.
- [26] POLETTTO, M.; PISTOR, V.; ZATTERA, A.J. Structural characteristics and thermal properties of native cellulose. In: Cellulose – Fundamental Aspects; van de VEN, T.; GODBOUT, L. (edit.). Intech: Croácia, 2013.
- [27] POLETTTO, M.; ZATTERA, A.J. Materials produced from plant biomass. Part III: degradation kinetics and hydrogen bonding in lignin. **Materials Research**. Vol. 16, p. 1065-1070, 2013.
- [28] MOHAN, D.; PITTMAN Jr, C.U.; STEELE, P.H. Pyrolysis of wood/biomass for bio-oil: a critical review. **Energy & Fuels**. Vol. 20, p. 848-889, 2006.
- [29] TELMO, C.; LOUSADA, J. The explained variation by lignin and extractive contents on higher heating value of wood. **Biomass & Bioenergy**. Vol. 35, p. 1663-1667, 2011.
- [30] SHEBANI, A.N.; van REENEN, A.J.; MEINCKEN, M. The effect of wood extractives on the thermal stability of different wood species. **Thermochimica Acta**. Vol 471, p. 43-50, 2008.
- [31] SHESHMANI, S.; ASHORI, A.; FARHANI, F. Effect of extractives on the performance properties of wood flour-polypropylene composites. **Journal of Applied Polymer Science**, Vol.123, p. 1563-1567, 2012.
- [32] SHEBANI, A.N.; van REENEN, A.J.; MEINCKEN, M. The effect of wood extractives on the thermal stability of different wood-LLDPE composites. **Thermochimica Acta**. Vol 481, p. 52-56, 2009.

[33] SANTANA, M.A.E.; OKINO, E.Y.A. Chemical composition of 36 Brazilian Amazon forest wood species. **Holzforschung**. Vol 61, p. 469-477, 2007.

[34] MÉSZÁROS, E.; JAKAB, E.; VÁRHEGYI, G. TG/MS, Py-GC/MS and THM-GC/MS study of the composition and thermal behavior of extractive components of *Robina pseudoacacia*. **Journal of Analytical and Applied Pyrolysis**. Vol 79, p. 61-70, 2007.

[35] BRASIL, MINISTÉRIO DO MEIO AMBIENTE. Levantamento sobre a geração de resíduos provenientes da atividade madeireira e proposição de diretrizes para políticas, normas e condutas técnicas para promover o seu uso adequado. Projeto PNUD BRA 00/20, 2009. Disponível em <[http://www.mma.gov.br/estruturas/164/\\_publicacao/164\\_publicacao10012011032535.pdf](http://www.mma.gov.br/estruturas/164/_publicacao/164_publicacao10012011032535.pdf)>.

[36] YANG, H.; YAN, R.; CHEN, H.; LEE, D.H.; ZHENG, C. Characteristics of hemicellulose, cellulose and lignin pyrolysis. **Fuel**. Vol 86, p. 1781-1788, 2007.

[37] POPESCU, M-C; POPESCU, C-M; LISA, G.; SAKATA, Y. Evaluation of morphological and chemical aspects of different wood species by spectroscopy and thermal methods. **Journal of Molecular Structure**. Vol 988, p. 65-72, 2011.

[38] POPESCU, C-M; SINGUREL, G.; POPESCU, M-C; VASILE, C.; ARGYROPOULOS, D.S.; WILLFÖR, S. Vibrational spectroscopy and X-ray diffraction methods to establish the differences between hardwood and softwood. **Carbohydrate Polymers**. Vol 77, p. 851-857, 2009.

[39] POPESCU, C-M; POPESCU, M-C; SINGUREL, G.; VASILE, C.; ARGYROPOULOS, D.S.; WILLFÖR, S. Spectral characterization of Eucalyptus wood. **Applied Spectroscopy**. Vol 61, p. 1168-1177, 2007.

- [40] GUO, X-J.; WANG, S-R.; WANG, K-G.; LIU, Q.; LUO, Z-Y. Influence of extractives on mechanism of biomass pyrolysis. **Journal of Fuel Chemistry and Technology**. Vol 38, p. 42-46, 2010.
- [41] TENORIO, C.; MOYA, R. Thermogravimetric characteristics, its relation with extractives and chemical properties and combustion characteristics of ten fast-growth species in Costa Rica. **Thermochemica Acta**. Vol 563, p. 12-21, 2013.
- [42] SLOPIECKA, K.; BARTOCCI, P.; FANTOZZI, F. Thermogravimetric analysis and kinetic study of poplar wood pyrolysis. **Applied Energy**. Vol 97, p. 491-497, 2012.
- [43] POLETTI, M.; DETTERBORN, J.; PISTOR, V.; ZENI, M.; ZATTERA, A.J. Materials produced from plant biomass. Part I: evaluation of thermal stability and pyrolysis of wood. **Materials Research**. Vol. 13, p. 375-379, 2010.
- [44] YAO, F.; WU, Q.; LEI, Y.; GUO, W.; XU, Y. Thermal decomposition kinetics of natural fibers: activation energy with dynamic thermogravimetric analysis. **Polymer Degradation and Stability**. Vol. 93, p. 90-98, 2008.
- [45] SHEN, D.K.; GU, S.; JIN, B.; FANG, M.X. Thermal degradation mechanisms of wood under inert and oxidative environments using DAEM methods. **Bioresource Technology**. Vol. 102, p. 2047-2052, 2011.
- [46] SANCHEZ-SILVA, L.; LÓPEZ-GONZÁLEZ, D.; VILLASEÑOR, J.; SÁNCHEZ, P.; VALVERDE, J.L. Thermogravimetric-mass spectrometric analysis of lignocellulosic and marine biomass pyrolysis. **Bioresource Technology**. Vol. 109, p. 163-172, 2012.
- [47] MAMLEEV, V.; BOURBIGOT, S.; YVON, J. Kinetic analysis of the thermal decomposition of cellulose: the main step of mass loss. **Journal of Analytical and Applied Pyrolysis**. Vol 80, p. 151-165, 2007.

- [48] CAPART, R.; KHEZAMI, L.; BURNHAM, A.K. Assessment of various kinetic models for the pyrolysis of a microgranular cellulose. **Thermochemica Acta**. Vol 417, p. 79-89, 2004.
- [49] KIM, U-J., EOM, S.H.; WADA, M. Thermal decomposition of native cellulose: Influence on crystallite size. **Polymer Degradation and Stability**. Vol 95, p. 778-781, 2010.
- [50] WANG, J.; WANG, G.; ZHANG, M.; CHEN, M.; LI, D.; MIN, F.; CHEN, M.; ZHANG, S.; REN, Z.; YAN, Y. A comparative study of thermolysis characteristics and kinetics of seaweeds and fir wood. **Process Biochemistry**. Vol 41, p. 1883-1886, 2006.
- [51] YORULMAZ, S.Y.; ATIMTAY, A.T. Investigation of combustion kinetics of treated and untreated waste wood samples with thermogravimetric analysis. **Fuel Processing Technology**. Vol 90, p. 939-946, 2009.
- [52] BIANCHI, O.; DAL CASTEL, C.; de OLIVEIRA, R.V.B.; BERTUOLI, P.T.; HILLIG, E. Avaliação da degradação não-isotérmica de madeira através de termogravimetria – TGA. **Polímeros**. Vol 20, p. 395-400, 2010.
- [53] ORNAGHI Jr., H.L.; POLETTO, M.; ZATTERA, A.J.; AMICO, S.C. Correlation of the thermal stability and the decomposition kinetics of six different vegetal fibers. **Cellulose**. Vol 21, p. 177-188, 2014.
- [54] DAHIYA, J.B.; KUMAR, K.; MULLER-HAGEDORN, M.; BOCKHORN, H. Kinetics of isothermal and non-isothermal degradation of cellulose: model-based and model-free methods. **Polymer International**. Vol 57, p. 722-729, 2008.
- [55] POLETTO, M.; PISTOR, V.; ZENI, M.; ZATTERA, A.J. Crystalline properties and decomposition kinetics of cellulose fibers in wood pulp obtained by two pulping processes. **Polymer Degradation and Stability**. Vol 96, p. 679-685, 2011.

[56] TAPPI T 204 cm-97. Solvent extractives of wood and pulp. Atlanta: Tappi Press, 1997.

[57] TAPPI T 222 om-02. Acid-insoluble lignin in wood and pulp. Atlanta: Tappi Press, 2002.